Standardised methods for the determination of key performance indicators for latent thermal energy storage heat exchangers

Beyne, W.[a,b *], T'Jollyn, I.[a,b], Lecompte, S.[a,b], Cabeza, L.F.[c], De Paepe, M.[a,b]

[a] Department of Electromechanical, Systems and Metal Engineering, UGent, Ghent, Belgium

[b] FlandersMake@UGent – Core lab EEDT-MP, Leuven, Belgium

[c] GREiA Research Group, Universitat de Lleida, Pere de Cabrera s/n, 25001 Lleida, Spain

*corresponding author, wim.beyne@ugent.be

Abstract

Latent thermal energy storage (LTES) heat exchangers can improve a diverse range of energy systems which has resulted in a large amount of work on the topic. However, it is difficult to compare studies on LTES heat exchangers due to a lack of standardized methods to characterize the performance of these systems. The present paper reviews the characterization methods found in literature and presents a thermodynamic framework for classifying the reported performance indicators. The averaged effectiveness-number of transfer units (ε-NTU) and phase change time method are identified as important predictive models, analyzed, and compared based on their theoretical derivation. The relation between the averaged effectiveness and phase change time is investigated both theoretically and based on data available in literature which results in recommendations for standardizing the characterization of LTES heat exchangers. By standardizing characterization of LTES heat exchangers, researchers can assess the performance of LTES heat exchangers in different energy systems without additional experiments or CFD calculations.

Keywords: latent thermal energy storage, heat exchanger, effectiveness-number of transfer units, solidification/melting time, (dis)charging time, charging time energy fraction

Word count: 13778

Highlights:

- A thermodynamic framework is developed.
- Based on the framework, reported performance indicators are categorized.
- Predictive models for phase change time and effectiveness are derived.

Nomenclature

Symbol	Description	Units
a	Fitting constant	kg/(K m² s) or Ks
A	Area	m²

b	Fitting constant	kg/(m² s) or K kg
c	Fitting constant	s
C	Fitting constant	kg/(m²s)
c_p	Specific heat capacity	J/(kg K)
d	Fitting constant	s/kg or kg
E	Energy	J
f	function	Varies
F	Integrated efflux of energy	J
$\dot{F}$	Efflux of energy	W
g	Gravitational constant	m/s²
h	Specific enthalpy	J/kg
J	Stored energy	J
K	Overall heat transfer coefficient per unit of surface area	W/(m² K)
KA	Overall heat transfer coefficient	W/K
KP	Overall heat transfer coefficient per unit of length	W/(m K)
m	Mass	Kg
$\dot{m}$	Mass flow rate	kg/s
P	Perimeter	M
$\dot{Q}$	Heat	W
T	Temperature	K
ΔT_0	Temperature difference between phase change temperature and HTF at the inlet of the heat exchanger.	K
ΔT_L	Temperature difference between phase change temperature and HTF at the outlet of the heat exchanger.	K
ΔT_{LM}	Logarithmic mean temperature difference	K
t	Time	S
t_0	Time required for the PCM to undergo complete phase change at the inlet of the HTF.	S
t_c	Time duration based on stored energy level	S
t_{ini}	Initial time	S
t_L	Time required for the PCM to undergo complete phase change at the inlet of the HTF. Total phase change time.	S
t_{pc}	Time duration based on total liquid fraction level	S
t_x	Time instant	S
U	Internal energy	J
ΔU	Internal energy change between two uniform temperatures	J
ΔU_A	Internal energy change per unit of length	J/m
v	Velocity	m/s
V	Volume	m³
$\dot{W}$	Work	W
x	Position along the bulk flow path of the HTF	M
$\vec{x}$	Position	Vector [m]
z	Height	M
Greek		
α	Energy fraction	[-]
ε	Effectiveness	[-]
$\bar{\varepsilon}$	Time averaged effectiveness	[-]
$\bar{\varepsilon}_{\bar{\lambda}}$	Liquid fraction averaged effectiveness	[-]

η_{fin}	Fin efficiency	[-]
λ	Local liquid fraction	[-]
$\bar{\lambda}$	Total liquid fraction	[-]
λ_A	Liquid fraction averaged over surface perpendicular to the bulk flow direction of the heat transfer fluid.	[-]

Acronym

C	Container
HTF	Heat Transfer Fluid
NTU	Number of Transfer Units
PCM	Phase change material

Scripts

in	Heat transfer fluid inlet	
ini	Initial value	
lat	Latent heat	
out	Heat transfer fluid outlet	
sens	Sensible heat	
$\bar{a}_b$	*a* averaged over *b*. If *b* is not specified then a time average.	Units of *a*

1. Introduction

Latent thermal energy storage (LTES) systems are being implemented in energy systems such as buildings [1-5], construction materials [6, 7], cold chain storage [8, 9], domestic hot water storage [10, 11], grid level power storage [12, 13] and solar energy [14, 15]. To implement LTES heat exchangers, they first need to be designed. The design process can be split into three steps [16]. The first step is the selection of a phase change material. The phase change temperature should correspond to the required temperatures for the application while the specific enthalpy should be as high as possible. A second step is ensuring the compatibility and stability of phase change materials (PCM) and enclosure materials. A third step is the geometric design and sizing of the heat transfer area between the storage material and the heat sources and sinks.

A large amount of materials have been tested in literature to use as PCM and research continues on novel materials for high temperature use [17-20]. Some PCMs are commercially available in the temperature range of -100 °C to 885 °C [21-23]. The selection of a PCM as storage material is discussed in general by Mehling and Cabeza [24] or more recently by Farid et al. [25] and for specific temperature ranges by Nie et al. [26] or Liu et al. [27]. Material selection will therefore be left out of scope of the present paper.

The second selection step concerns the compatibility of PCMs with their container. In general, material compatibility depends on the type of PCM. Materials used for LTES were first classified by Abhat [28] in 1983 as organic (based on carbon) or inorganic (based on salts) substances. Later on, eutectic mixtures of organic-organic, inorganic-organic and inorganic-inorganic were added [29, 30]. In general, metals can suffer from corrosion when brought into contact with inorganic PCMs while plastics can be unstable in combination with organic PCMs or allow migration of both organic and inorganic PCM [31, 32]. The material compatibility of PCMs has been studied in more detail for applications such as cold storage [33], (molten) salts for concentrated solar power [34], plastics and PCMs [35] and PCMs for building applications [22]. For a more thorough review, the reader is referred to Rathod et al. [36] or more recently

Cardenas et al. [37]. In conclusion, the tools are available to investigate the compatibility of a PCM and a container material and the discussion will be out of the scope of this paper.

The third step is the geometrical design of the LTES system. Mehling and Cabeza [24] identified three geometry types based on the energy transfer method from storage material to system: by heat transfer on the storage surface, by heat transfer on internal heat transfer surfaces, and by transferring the heat storage material itself. The present review concerns LTES heat exchangers i.e., LTES systems with heat transfer on an internal system through a heat transfer fluid.

When researching LTES heat exchanger design, many authors focus on enhancing the thermal performance of the PCM. Tao and He [38], Al-Maghalseh and Mahkamov [39] and Lin et al. [40] all review heat transfer enhancement in LTES systems in general. Several authors also review specific enhancement techniques. Wong-Pinto et al. [41] reviewed nano-enhancement of salt hydrates. Zhang et al. [42] reviewed shape stabilized PCMs based on porous matrices. Jiang et al. [43] reviewed the combination of porous materials and inorganic salts above 200 °C and Feng et al. [44] and Zhang et al. [45] focused on porous materials on micro or nanoscale. Abdulateef et al. [46] review the effects of fin geometry on LTES systems. There are thus several options for designing and enhancing LTES heat exchangers which raises the question how the performance of LTES systems can be characterized and compared. The LTES heat exchangers are essentially standard heat exchangers where one of the working fluids has been replaced with a stationary storage material [16]. Therefore, it is interesting to investigate the methods used to design and characterize a standard heat exchanger. The goal of these methods is determining the outlet temperature of the heat transfer fluid (HTF) streams given the inlet temperatures and mass flow rates [47, 48]. The design methods for heat exchangers are based on either the logarithmic mean temperature difference (LMTD) or the effectiveness-number of transfer units (ϵ-NTU) method. Based on the LMTD or ϵ-NTU method, an overall heat transfer coefficient can be used to characterize the performance of heat exchangers operating in steady state.

The difference between LTES heat exchangers and standard heat exchangers is that LTES heat exchangers do not operate at steady state. The energy content of LTES heat exchangers changes during charging and discharging since they are energy storage systems. In contrast, standard heat exchangers can be analyzed under steady-state conditions. The transient operation of LTES heat exchangers leads to two challenges compared to standard heat exchangers: the definition of performance indicators and development of predictive models.

In steady-state operation, the state of the HTF at the outlet of a heat exchanger is constant in time. Performance indicators for the operation of standard heat exchangers are thus scalars such as the pressure drop or the outlet temperature of the two HTF streams [48]. In contrast, describing the operation of a LTES heat exchanger involves the state of the LTES heat exchanger and the state of the HTF at the outlet as a function of time. The important aspect of the time functions describing the operation of the LTES heat exchanger is thus determined by its use in the system into which the LTES heat exchanger is integrated. As a result, a wide variety of performance indicators (PIs) are reported depending on the application [49].

Designing or characterizing a heat exchanger requires creating predictive models for the performance indicators. When designing a standard heat exchanger, the overall heat transfer coefficient is determined which can then be used to determine the outlet temperatures through either the LMTD or ϵ-NTU method [48]. Similarly when characterizing an existing heat exchanger, the overall heat transfer coefficient is

measured through methods such as the Wilson plot method [50] which require the application of the LMTD or ϵ-NTU method. Since the LMTD and ϵ-NTU method are not applicable to LTES heat exchangers, there is no general method for creating a predictive model for performance indicators.

The transient operation of LTES heat exchangers has thus resulted in a wide variety of reported PIs without a general method of obtaining predictive models. This issue applies more broadly to TES in general and efforts to select and categorize key performance indicators (KPI) for TES have been developed within the IEA-ECES Annex 30 [51]. The resulting approach is disseminated both by Gibb et al. [52] and Palomba et al. [53]. In this approach, KPIs are identified in three steps. In the first step, the TES system is characterized which results in the TES *system parameters*. In the second step, the performance of the TES system in the full process is analyzed considering any external factors to the full process. In this step, the TES system is analyzed taking into account the application into which it is implemented which results in the selection of the relevant *performance parameters*. In the third step, KPIs are selected from the performance indicators depending on the stakeholders' perspectives. The presented approach thus leads to three types of parameters:

- System parameters: determined from the TES system only.
- Performance indicators: describe the performance of the TES system in the process.
- Key performance indicators: selection of the important performance indicators based on the stakeholder perspective.

Palomba et al. [53] present a categorization of PIs. The PIs are split into three major categories: technical, economic, and life cycle PIs. The technical performance indicators relate to physical quantities such as mass, energy, or volume. The economic PIs on the other hand relate to the cost, income or savings realized for the process into which the TES system is integrated. The economic PIs can be presented in relation to technical PIs, e.g., the specific investment cost of the storage system is defined by the ratio of the investment cost and the stored energy. Life cycle PIs relate to the impact of the TES system on the environment in which all stages of the TES system life cycle are considered.

In the present paper the technical PIs are the focus. In the next section, a novel thermodynamic framework is defined to scope the discussion and present reported technical performance indicators in a unified way. In the third section, the literature on technical performance indicators is reviewed. In the fourth section, the predictive models for the effectiveness-NTU relation and phase change time for LTES heat exchangers are derived and analyzed. To the authors knowledge, the derivation for the effectiveness method is the only rigorous derivation in literature specifically for LTES heat exchangers. Furthermore, the derivation of the phase change time is the most general version of the derivation which can be found. A final important novelty is that the thermodynamic framework allows to compare characterizing through the effectiveness method or through the phase change time method.

2. Thermodynamic framework

The thermodynamic framework presented in this section is split into three major parts. First, thermal energy storage is defined based on the first law of thermodynamics. Second, a novel technical performance classification is proposed. Third, the methods required to determine the performance indicators are described.

2.1. Thermal energy storage definition

A thermodynamic framework for LTES heat exchangers requires a clear definition of LTES and therefore of TES. The term TES is often defined by summing up types of TES rather than stating a definition (e.g., Dincer and Rosen [54]). The effort is made to find a definition which is both sound from a thermodynamics point of view and which includes storage systems which are commonly classified as TES.

The definition for TES will be based on a closed thermodynamic system. This allows expressing the first law of thermodynamics as Equation 1 which will form the basis for the TES definition:

$$\frac{dE}{dt} = \dot{Q} - \dot{W} \qquad 1$$

The definition is split in two steps. In a first step an energy storage system is defined as:

A closed thermodynamic system which undergoes a cycle in three steps: charging, storing, and discharging.

- *In the charging step, the energy of the system is changed from E_0 to E_1.*
- *In the storing step, the energy of the system can change from E_1 to E_2 with $|E_1\text{-}E_0| \geq |E_2\text{-}E_1|$.*
- *In the discharging step, the energy of the system is changed from E_2 to E_0.*

The definition of energy storage does not state whether the energy after the charging step E_1 is greater than the initial energy E_0. Otherwise, ice storage systems would not be regarded as energy storage. The storing step condition implies that part of the stored energy difference $E_1\text{-}E_0$ is potentially lost. The discharging step returns the storage system to its initial energy E_0 which closes the cycle.

In the second step, a thermal energy storage system is defined:

A thermal energy storage system is an energy storage system which cannot apply work on its surroundings during the discharging step except for volume change work.

The definition only limits energy transfers during the discharging phase. The thermal energy storage can thus be charged through a work input. Therefore, the definition includes sensible TES systems using rocks which are charged with resistive heaters (e.g., [57]).

The thermal energy storage system can apply volume work on its surroundings. The system is thus free to expand and contract due to charging and discharging which allows for the thermal expansion of storage materials.

Many systems which are regarded as thermal energy storage are open systems. In this case, the first law of thermodynamics is given by Equation 2:

$$\frac{dE}{dt} = \dot{Q} - \dot{W} + \sum_{inlet} \dot{m}\left(h + \frac{v^2}{2} + gz\right) - \sum_{outlet} \dot{m}\,(h + \frac{v^2}{2} + gz) \qquad 2$$

The difference between the first law applied to a closed system and an open system is the energy transfer associated with mass in- and outflow: $\sum_{inlet} \dot{m}\left(h + \frac{v^2}{2} + gz\right) - \sum_{outlet} \dot{m}\,(h + \frac{v^2}{2} + gz)$. Formally expanding the definition to open systems thus requires additional requirements on this energy transfer associated with mass flow. This is not trivial since an enthalpy difference or a difference in state are

independent of the path to go from one state to another. Therefore, enthalpy differences cannot simply be associated with only heat.

Instead of formally expanding the definition, a more practical approach is taken. Open systems can be analyzed as thermal energy storage systems by interpreting the energy transfer associated with mass flow by a heat transfer. This is akin to how gas power cycles are interpreted as power cycles [58].

2.2. Performance indicator classification

The present paper is about latent thermal energy storage heat exchangers with solid-liquid phase change. Figure 1 gives a schematic overview of a LTES heat exchanger with a control volume for the expression of the conservation of energy. The difference in potential and kinetic energy between inlet and outlet can be assumed negligibly small compared to the internal energy difference. Furthermore, there is no work except for flow work. Finally, a single inlet and outlet are assumed. The first law of thermodynamics reduces to Equation 3 where *U* is the internal energy of the storage, and $\dot{Q}_{loss}$ is the heat loss or gain over the boundaries of the control volume.

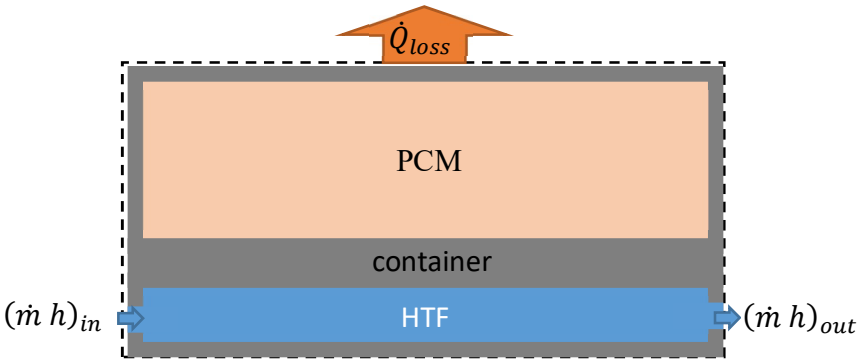

Figure 1: Schematic overview of a LTES heat exchanger. The control volume used to express Equation 3 is shown in dashed lines.

$$\frac{dU}{dt} = \dot{Q}_{loss} + (\dot{m}h)_{in} - (\dot{m}h)_{out} \quad (3)$$

Equation 3 can be integrated in time to result in Equation 4 where J is the stored internal energy change up to time t (Equation 5), Q_{loss} are the total heat losses up to time t and F is the integrated efflux of energy up to time t starting from the initial time t_{ini} (Equation 6). The efflux of energy is the energy transfer associated with the mass flux in and out of the control volume [59]. The information in Equation 3 can be translated to the information in Equation 4 while differentiation allows translating Equation 4 into Equation 3. Both expressions of the first law are thus equivalent.

$$J(t) = Q_{loss}(t) + F(t) \quad (4)$$

$$J(t) = \int_{t_{ini}}^{t} \frac{dU}{dt} dt = U(t) - U(t_{ini}) \quad (5)$$

$$F(t) = \int_{t_{ini}}^{t} [(\dot{m}h)_{in} - (\dot{m}h)_{out}]\, dt \quad (6)$$

The novel classification proposed in this paper of technical performance indicators is based on the conservation of energy as expressed in Equation 3 and 4. The novel categorization allows to focus on the challenges faced when determining the indicator and the connection between indicators.

The first type of indicators are functions of the thermodynamic state of the storage system only and will be designated time-independent state indicators. They describe the state of the storage system in between the charging, storing, and discharging processes. Examples are the geometry of the storage system, the mass of the individual components but also the equations of state for the materials constituting the storage system.

The second type of indicators concerns a part of the storage cycle (either charging, storage, or discharging) and are thus described by Equation 3. These process indicators are further subdivided into three subcategories. The first subcategory considers the state of the system during the process or the left-hand side of Equation 3. The second subcategory concerns the energy transfers between the LTES system and the environment or the right-hand side of Equation 3. The third subcategory describes the duration of the processes. They are the link between energy and transfer indicators.

The new categories can be summarized as follows:

- Time-independent state indicators
- Process indicators
    - State indicators
    - Energy transfer indicators
    - Time indicators

The time-independent state indicators are readily available from the geometry of the heat exchanger and the properties of the materials present in the storage system. In the framework of Gibb et al. [52] these indicators are system indicators. Determining a predictive model for these indicators is thus purely a question of material characterization. Material characterization of PCMs is a specialized topic [1, 37, 60, 61], however once a material is characterized it can be used in different LTES systems. The issue of characterizing time-independent state indicators can thus be separated from the characterization of process indicators and will be left out of scope of the present discussion.

In the indicator framework described by Gibb et al. [52], the distinction between KPI and PI stems from the stakeholder perspective on the performance of the LTES heat exchanger [52]. The performance of the LTES heat exchanger is determined by its interactions with the energy system into which it is integrated. The interaction of a LTES heat exchanger is determined by the energy transfers or the right-hand side of Equation 3. Therefore, only the energy transfer and time indicators can be KPIs while the state indicators cannot be KPIs.

Although state indicators will not be KPIs, they have value to report since they can increase the understanding of a charging cycle (e.g., [62]), be used to validate numerical code (e.g., [63-66]), or hold predictive value for energy transfer and time indicators (e.g., [67]).

The three types of process technical performance indicators all hold reporting value as they can either be KPIs or allow predicting them. The next section deals first with determining and measuring the three types of process performance indicators. Furthermore, the reported indicators in literature are discussed.

3. Process performance indicators

The next paragraphs contain a summary of the process indicators reported by a selection of articles found on the Web of Science database for the key words *Latent Thermal Energy Storage* and *heat exchanger*. The indicators are grouped according to the classification developed in Section 2.

Indicators which are ratios of separate indicators will not be discussed separately since the challenge of determining these indicators is equivalent to determining several separate single process indicators. Examples of such indicators are the stored energy in the PCM divided by the phase change time [68] or the stored energy in the PCM divided by the total stored energy [69] or the average efflux of energy divided by the stored energy [70]. Other examples of such ratios are specific to a heat source or sink such as solar storage efficiency [71] or daily efficiency [72]. These heat source or sink dependent indicators will not be discussed. Several authors define an energy [73, 74] or exergy efficiency [75, 76] as the integrated efflux of energy divided by the total pumping work. The present paper does not consider the pumping work and therefore these definitions will not be discussed. An alternative definition for the exergetic efficiency can be based on the exergy of the HTF stream compared to the exergy in the PCM [77]. The stored exergy is not considered in this paper.

3.1. State indicators

The process state indicator concerns the time derivative of the internal energy of the LTES heat exchanger. A LTES heat exchanger consists of three materials: heat transfer fluid (HTF), the container (C), and the storage material or phase change material (PCM). Accordingly, the left-hand side of Equation 4 can be split into three parts (Equation 7):

$$J = J_{HTF} + J_{PCM} + J_c \qquad 7$$

The stored energy in HTF, PCM, and container is the difference in internal energy between time t and the initial time t_{ini} (see Equation 5). The internal energy can be determined by integrating the specific internal energy as a function of the local state $State(\vec{x}, t)$ over the mass of the constituent material (HTF, PCM, or container). The control volumes over which the integration is performed are shown schematically in Figure 2.

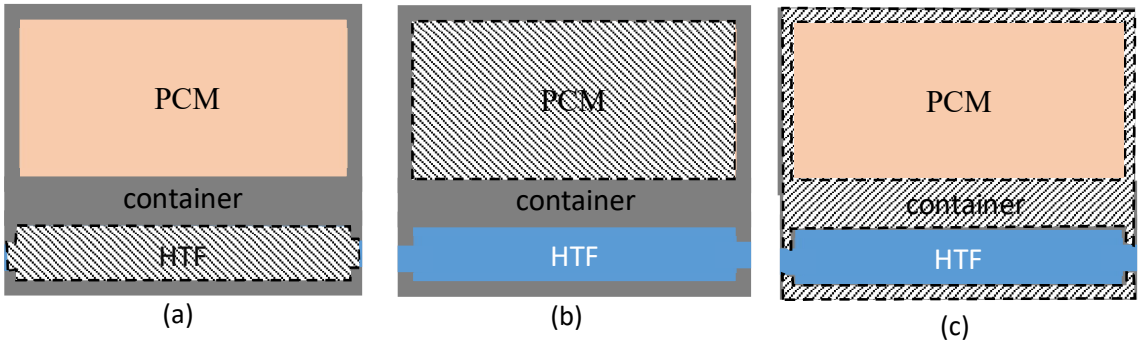

Figure 2: Schematic representation of a LTES heat exchanger with an indication of the integration volumes used to express Equation 8 (a), Equation 9 (b) and Equation 10 (c).

In the case of the HTF, the mass in the LTES heat exchanger is not necessarily constant due to thermal expansion. The HTF thus needs to be integrated over the volume (Equation 8) while the PCM and container need to be integrated over the mass (Equation 9 and 10):

$$U_{HTF}(t) = \int_{HTF} u_{HTF}\big(State(\vec{x},t)\big)\rho_{HTF}(State(\vec{x},t))dV \quad (8)$$

$$U_{PCM}(t) = \int_{PCM} u_{PCM}\big(State(\vec{x},t)\big)dm \quad (9)$$

$$U_{C}(t) = \int_{C} u_{C}\big(State(\vec{x},t)\big)dm \quad (10)$$

Equations 8-10 show that state indicators are functions of the local state and the specific internal energy (and density) as a function of the state. The specific internal energy as a function of the state is a time independent indicator and can be determined by material characterization. If these functions are known, determining state indicators for a (dis)charging process is equivalent to determining the local state as a function of time. Determining the state of a pure fluid in a simple compressible system, requires determining two independent properties [78]. Further assumptions allow to reduce the requirement of two independent properties.

The container material is a solid and is therefore assumed to be incompressible. Only the temperature is required to fix the state.

The PCM is in a solid and/or liquid state throughout the (dis)charging process. Therefore, it is most often assumed to be incompressible. For an incompressible material, the internal energy of the material is a function of the temperature and the phase-state [78]. The phase is most often expressed as a liquid (or solid) fraction or the ratio of the PCM mass which is liquid (or solid) to the total PCM mass [24].

The liquid fraction can be measured using both local and global techniques [79]. Local techniques are based on a measurable property which changes with the phase fraction. Examples of such properties are electrical properties (resistive, capacitive, or inductive) [80], transmissivity of light or ultrasonic waves [80], or temperature [81, 82]. In a sufficiently dense grid, these local measurements can provide a total liquid fraction estimate [79]. Global techniques in contrast require only a single measurement to determine the total liquid fraction. These techniques are based on visually assessing the phase change front (e.g., [83]), a density change between solid and liquid state (e.g., [67]) or even the sound damping properties of the LTES heat exchanger [84]. In any case, there is no generally applicable method for measuring local or total liquid fraction and the choice depends on PCM properties and heat exchanger geometry [79].

The HTF can be both liquid (e.g., [8]), gas (e.g., [85]) or liquid-gas (e.g., [86]). Incompressibility can usually be assumed for liquid HTF resulting in only the temperature being required to determine the internal energy. For gasses, ideal gas behavior can often be assumed in which case only a temperature measurement is required to determine internal energy [78]. Only in the liquid-gas phase or for non-ideal gasses, an additional independent state variable is required to fix the HTF phase.

Determining the state indicators of a process thus requires determining the local temperature $T(\vec{x},t)$ and local $\lambda(\vec{x},t)$ or total $\bar{\lambda}(t)$ liquid fraction as a function of time. Only in a limited number of papers, additional state variables are required to fix the state of the HTF.

Both local temperatures and liquid fraction and total liquid fraction are reported in experimental [63, 64, 67, 69, 72, 76, 83, 87-118] and numerical [63-66, 68, 70, 71, 75, 77, 93, 98, 99, 102, 104, 106, 109, 111, 113, 115, 119-136] studies. A key difference between the experimental and numerical studies is the sampling density in space for both temperature and liquid fraction. Numerical studies can report local temperatures and liquid fractions at specific locations (e.g., [65, 98, 104, 122, 123]) or map temperatures and liquid fraction for each node (e.g., [65, 66, 68, 98, 99, 104, 119, 122]). Often, the local PCM temperatures are used to validate numerical results with experimental measurements (e.g., [65, 98, 104, 122, 129, 130]). In contrast, experimental studies are limited to discrete sensor locations (e.g., [63, 64, 69, 72, 83, 87-104, 108-118]) or global liquid fraction techniques (e.g., [87, 101]).

The difference in spatial sampling results in a difference in papers which report the internal energy. In numerical studies reporting internal energy as a function of time is commonly done although most studies report latent stored internal energy (e.g., [71, 99, 104, 130]) or total liquid fraction (e.g., [65, 66, 68, 70, 71, 75, 77, 93, 99, 102, 104, 106, 109, 111, 113, 115, 120-122, 124-128, 130-132, 134, 136]) instead of total stored energy (e.g., [75, 111, 115, 134, 137, 138]). In experimental studies, the total liquid fraction is sometimes reported (e.g., [67, 87, 101]) however local temperature measurements are far more commonly reported (e.g., [63, 64, 69, 72, 76, 83, 87-103, 105-118]). A limited number of experimental studies also present internal energy change as a function of time (e.g., [76, 83, 89, 101, 105, 114, 116]) with two studies [89, 105] estimating energy stored in HTF, container and PCM separately and one study estimating the internal energy change in the HTF, container and PCM during storage periods [139].

The local temperature and liquid fraction can be used to define statistics. Chen et al. [136] report both the mean and standard deviation of the temperature and liquid fraction. The statistics are used to describe the melting rate uniformity. The mean or bulk PCM temperature is also reported by several authors (e.g., [108, 125, 130, 140]).

Besides change of internal energy, several authors define ratios such as the storage efficiency (ratio of stored energy to solar irradiance) [71], internal energy change of the PCM to melting time [68], and the internal energy change of the PCM compared to the total energy change [69]. Although these ratios are valuable for understanding the operation to LTES heat exchangers they do not lead to predictive models for PIs.

In conclusion, most numerical studies focus on the latent internal energy while most experimental studies are limited to presenting local temperature measurements. However, state indicators are only valuable if they allow predicting energy transfer or time indicators according to the KPI framework discussed in Section 2. Regarding the conservation of energy expressed in Equation 3, the internal energy change of both the HTF, container and PCM is required to estimate energy transfer indicators. As a result, most studies are not able to link energy transfer with state estimators and therefore do not lead to predictive models of KPIs. To summarize the studies in this section, all reported state indicators are shown in Table 1.

Table 1: Summary of the reported process state indicators.

Parameter	Name	Numerical	Experimental

U	Internal energy	[75, 111, 115, 134, 137, 138]	[76, 83, 89, 101, 105, 114][116]
U_{HTF}	Internal energy HTF		[89, 105]
U_C	Internal energy container		[89, 105]
U_{PCM}	Internal energy PCM	[99, 104, 137]	[89, 141]
U_{sens}	Internal sensible energy PCM	[71, 104, 130, 138]	[105, 114]
U_{lat}	Internal latent energy PCM	[71, 104, 130, 138]	[105, 114]
$\lambda(\vec{x},t)$	Local liquid fraction	[65, 66, 68, 70, 71, 75, 98, 99, 102, 104, 119, 122, 123, 142][77, 106, 109, 125, 127-135]	[83, 87, 94, 104] [114]
$\bar{\lambda}(t)$	Overall liquid fraction	[65, 66, 68, 70, 71, 75, 77, 93, 99, 102, 104, 106, 109, 111, 113, 115, 120-122, 124-128, 130-132, 134, 136]	[87, 101]
$T(\vec{x},t)$	Local temperature	[125-130]	[76, 105-107]
PCM	Local PCM temperature	[63-66, 68, 70, 71, 75, 77, 93, 98, 99, 104, 109, 115, 119-121, 131-135, 143, 144]	[63, 64, 69, 72, 83, 87-103, 108-111, 143, 145-151][112-117]
Container	Local container temperature	[121, 143]	[100, 101, 118]
HTF	Local HTF temperature	[70, 71, 111, 123, 131, 134, 135, 143]	[65, 66, 96, 98, 99, 110, 116]

3.2. Energy transfer indicators

As can be seen in Equation 3 and 4, there are two types of energy transfer indicators: heat transfer to the ambient and efflux of energy.

3.2.1. Efflux of energy

Determining the efflux of energy requires measuring the mass flow rate of the HTF and determining the inlet and outlet state of the HTF. Determining the inlet and outlet state of the HTF is a simplified version of determining the thermodynamic state of the HTF and therefore already discussed above.

The mass flow rate, in-, and outlet temperature of the HTF are some of the most accessible measurements for LTES heat exchangers and are therefore often reported in experimental studies (e.g., [62, 63, 65, 66, 89, 91, 92, 95-97, 106, 123, 124, 141, 152]). Most authors calculate the efflux of energy (e.g., [62, 72, 76, 77, 83, 90, 92, 96, 97, 106, 108, 110, 117, 118, 124, 126, 152]), and some the integrated efflux of energy (e.g., [83, 87, 92, 95, 97, 100, 101, 103, 117, 126, 152]).

The efflux of energy is often averaged over time (e.g., [83, 90, 95-97, 117]), per unit of heat transfer area (e.g., [83]) or divided by the PCM mass [106] to compare LTES heat exchangers. Peak efflux of energy or

the ratio of peak efflux of energy to total internal energy change is also reported [95]. To the authors knowledge, only Tarragona et al. [62] determine a predictive model for the peak efflux of energy.

Several authors compare the integrated efflux of energy at the end of charging to the internal energy change of the heat exchanger between two temperatures (e.g., [8, 92, 103, 152]). In the case of negligible losses, both values should be equal which allows to link the efflux of energy to the total internal energy change through the conservation of energy (see Equation 3) (e.g., [8, 118, 152]).

The HTF outlet temperature is often characterize using a heat exchanger effectiveness [63, 64, 67, 91, 97, 103, 110, 119, 124, 138, 153]. However, different effectiveness definitions for LTES heat exchangers are used depending on the study. The fact that multiple definitions for effectiveness of LTES heat exchangers exist seems strange for the concept of effectiveness which is well established in classical heat transfer analysis of steady state heat exchangers. To understand why multiple definitions are possible for LTES heat exchangers, the classical concept of effectiveness for steady state heat exchangers needs to be investigated first.

The effectiveness is defined for steady-state heat exchangers as the ratio of the heat transfer rate to the maximum possible heat transfer rate (Equation 11). As a result, it is bound between zero and one.

$$\varepsilon_{steady\ state} = \frac{\dot{Q}}{\dot{Q}_{max}} \tag{11}$$

The heat transfer rate $\dot{Q}$ and maximum heat transfer $\dot{Q}_{max}$ rate are proportional to the actual and maximum efflux of energy. If the enthalpy difference between inlet and outlet is a linear function of temperature, the actual and maximum efflux of energy are the product of the specific heat capacity, the mass flow rate and respectively the temperature difference and maximal temperature difference between inlet T_{in} and outlet T_{out} and the maximal temperature at the outlet T_{out}^{max}. The maximal outlet temperature is the outlet temperature for an infinitely long heat exchanger. In this case the stream temperatures of the two HTF streams become equal on one side of the heat exchanger (Equation 12).

$$\varepsilon_{steady\ state} = \frac{T_{out} - T_{in}}{T_{out}^{max} - T_{in}} \tag{12}$$

There are two major differences between steady-state and TES heat exchangers which affect the use of this definition. The first difference is the interpretation of the efflux of energy as the heat transfer to the container. Equation 13 is the conservation of energy expressed on a control volume around the HTF (control volume shown on Figure 2b). In a steady-state heat exchanger, the rate of change of the internal energy of the HTF is zero. As a result, the heat transfer rate is equal to the efflux of energy. In LTES heat exchangers, the rate of change is not zero. As a result, the efflux is not equal to the heat transfer. This deviation is neglected by most authors (e.g. [116]) as only a limited number of authors estimate the HTF internal energy rate of change of the HTF (e.g., Martinelli et al. [89] and Beyne et al. [154]).

$$\frac{dU_{HTF}}{dt} = \dot{Q}_{HTF-container} + (\dot{m}h)_{in} - (\dot{m}h)_{out} \tag{13}$$

The second difference concerns the right-hand side of Equation 13. The heat transfer rate and outlet temperature of the heat exchanger are constant in time for steady-state heat exchangers. As a result, the effectiveness of a steady-state heat exchanger is a scalar which can be expressed as the ratio of the

temperature change of the HTF over the heat exchanger to the temperature change of the HTF over the heat exchanger if the heat exchanger was infinitely long. For TES heat exchangers, the outlet temperature and heat transfer rate are not constant in time. As a result, the effectiveness is not a scalar but a function of time for LTES heat exchangers.

The effectiveness of a LTES heat exchanger can be defined as the ratio of the efflux of energy to the maximum efflux of energy. This definition avoids having to measure the heat transfer rate between HTF and container as would be necessary for the definition according to Equation 11.

$$\varepsilon_{TES} = \frac{\dot{F}}{\dot{F}_{max}} \tag{14}$$

The efflux of energy of a LTES heat exchanger is a function of time. As a result, the effectiveness definition of Equation 16 is also a function of time. It is logical to define the maximal efflux of energy $\dot{F}_{max}$ not as a function but as a scalar value. An example of the outlet temperature for the solidification of a LTES heat exchanger is shown on Figure 3. The maximum efflux occurs at the start of the cycle when the outlet temperature of the HTF is equal to the initial temperature. For a constant specific heat capacity of the HTF, the effectiveness of an LTES heat exchanger is thus defined as Equation 15:

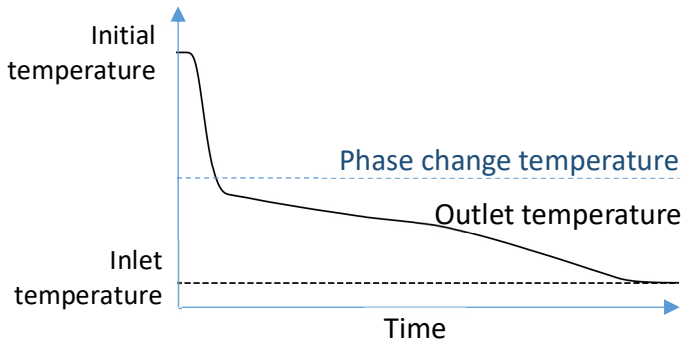

Figure 3: Schematic outlet temperature of a LTES heat exchanger during solidification.

$$\varepsilon_{ini} = \frac{T_{out} - T_{in}}{T_{ini} - T_{in}} \tag{15}$$

Effectiveness as defined by Equation 15 maintains the property that it is lower than 1 throughout the charging of the LTES heat exchanger. However, the reference temperature difference must be the driving force for heat transfer between the HTF and the container or PCM to derive a predictive relationship between effectiveness and number of transfer units. In LTES heat exchangers, the driving temperature difference for heat transfer changes during the (dis)charging since the temperature of the storage and container material change. The temperature difference in the case of Equation 15 is not the driving force for heat transfer except at the start of the cycle. Therefore, only a limited number of studies apply Equation 15 (e.g., [103, 110, 124]) and these studies do not result in a predictive model for the heat exchanger effectiveness.

The temperature difference between the (peak) phase change temperature and the HTF inlet is the driving temperature difference during the phase change. Since most research focusses on the outlet temperature during the phase change of the LTES heat exchanger, the effectiveness is often based on the temperature difference between inlet temperature and peak phase change temperature (Equation 16). Note that the effectiveness according to Equation 16 is no longer smaller than one throughout the entire charging cycle.

$$\varepsilon_{pc} = \frac{T_{out} - T_{in}}{T_{pc} - T_{in}} \quad 16$$

The effectiveness according to Equation 16 was first introduced by El-Dessouky and Al-Juwayhel [155] in a second law analysis for an annular tube LTES heat exchanger. In this study, the effectiveness is determined as a function of the number of transfer units (NTU) (Equation 17) as is done for steady-state heat exchangers with one of the heat transferring fluids at a constant temperature (Equation 18) [48]. The derivation of Equation 17 is done in Section 4. In the definition of the NTU (Equation 17), *KA* is the product of the overall heat transfer coefficient and the surface area:

$$NTU = \frac{KA}{\dot{m}c_p} \quad 17$$

$$\varepsilon_{pc} = 1 - \exp(-NTU) \quad 18$$

Ismail et al. [138] used the same effectiveness definition as Equation 16. However instead of using Equation 17 and 18, the effectiveness-NTU relation is directly determined from measurements by Equation 19 with ΔT_{LM} the logarithmic mean temperature difference. The logarithmic mean temperature difference method requires the same assumptions as the effectiveness-NTU method. As discussed before, equating the efflux of energy $\dot{F}$ to the heat transfer rate between HTF and PCM requires neglecting the internal energy change of the HTF.

$$NTU = \frac{\dot{F}}{\dot{m}c_p\,\Delta T_{LM}} \quad 19$$

The effectiveness defined by Equation 16 can be a function of the phase change fraction if the overall heat transfer coefficient *KA* is. Since the sensible heat of PCM and container are small, the overall heat transfer coefficient is determined by the convective heat transfer coefficient in the HTF, the conduction through the container wall and the heat transfer resistance from the container wall to the phase change front. This latter heat transfer resistance changes with the movement of the phase change front and thus it changes with the phase change fraction. In five studies [67, 142, 153, 156, 157], the effectiveness is determined as a function of the liquid fraction or a variable associated with the global liquid fraction $\bar{\lambda}$ (Equation 20):

$$\varepsilon_{pc} = f(\bar{\lambda}) \quad 20$$

The function $f(\bar{\lambda})$ is either experimentally measured [67, 156], analytically determined [153] or determined in a numerical study [142, 157]. In the analytic case, a phase change front shape is assumed which allows estimating the overall heat transfer coefficient and the effectiveness through Equation 18. In the experimental case, the effectiveness-liquid fraction curve is determined for separate mass flow rates.

Shen et al. [140] adapted the effectiveness definition based on the PCM temperature to a cascaded tube in tube LTES heat exchanger with 3 PCMs arranged along the flow length. Each PCM section is analyzed using a single control volume for the PCM and neglecting the internal energy change of the HTF. As a

result, the heat transfer rate can be described by an effectiveness-NTU relation using the bulk PCM temperature as a reference. Several studies determine an average effectiveness based on Equation 16 [63, 91, 97, 119, 145-147, 149, 150, 158]. This average effectiveness $\bar{\varepsilon}$ is derived by averaging the effectiveness over a time period between t_1 and t_2 as Equation 21:

$$\bar{\varepsilon} = \frac{1}{t_2 - t_1} \int_{t_1}^{t_2} \varepsilon_{pc}(t)\, dt \qquad 21$$

The average effectiveness requires specifying the averaging time period t_1 and t_2. In most studies, this time period is the phase change time of the charging cycle [91, 159]. The definition and measurement of phase change time is further discussed in the next section.

To the authors knowledge, average effectiveness was first defined by Sari and Kaygusuz [160] to characterize a tube-in-tube LTES heat exchanger. The effectiveness was reported for a single constant inlet temperature and mass flow rate and therefore no attempt at characterization could be made. Similarly to Sari and Kaygusuz [160], Tay et al. [119] used the concept to compare different fin geometries for a single operating point.

Castell et al. [91] determined a correlation for the average effectiveness as a function of mass flow rate and heat transfer surface area in a study on a shell and tube LTES heat exchanger. The effectiveness was averaged during the phase change time in the heat exchanger and compared for a single inlet temperature and different mass flow rates. Two designs were compared with a different tube length in the same shell based on the effectiveness as a function of the mass flow rate. The average effectiveness could be described as a function of the number of transfer units (NTU). By assuming the overall heat transfer coefficient to be the same for both design variants, the effectiveness could thus be determined as a function of the ratio of heat transfer surface and mass flow rate (Equation 22). In the case of Castell et al. [91], a polynomial was chosen to fit the data:

$$\bar{\varepsilon} = f\left(\frac{A}{\dot{m}}\right) \qquad 22$$

Tay et al. [159] expanded the work of Castell et al. [91] by studying the same shell and tube LTES heat exchangers with one, two and four tube banks, two different PCMs and melting and solidification cycles. Inspired by the ε-NTU relation given in Equation 18, the average effectiveness for all these cases can be expressed by a single correlation (Equation 23) with a value of 0.0199 for the fitting constant *C*:

$$\bar{\varepsilon} = 1 - \exp\left(-C\frac{A}{\dot{m}}\right) \qquad 23$$

Equation 23 allows sizing the shell and tube heat exchangers, since additional tube surface area is accounted for by the heat transfer surface area *A*.

In the work by Tay et al. [159], the fitting constant *C* is interpreted as a time averaged overall heat transfer coefficient $\overline{K}$. However, Equation 23 is not obtained when averaging the instantaneous effectiveness relation given by Equation 18 since the NTU and more specifically the overall heat transfer coefficient is a function of time. The constant *C* can only be interpreted as a time averaged overall heat transfer coefficient if the NTU is approximately constant as a function of time. However, the NTU is a function of the phase change front position which changes as a function of time. Therefore, the fitting coefficient C can only be interpreted as a time averaged overall heat transfer coefficient if the change in phase change

front position only has a minor effect on the NTU. In a follow up study on the same experimental setup [161], the thermal resistance of the HTF and container wall was shown to be dominant. Therefore, interpreting the fitting coefficient *C* being similar as the result of the heat transfer coefficient being similar is probably warranted in the case of Tay et al. [159].

Several authors used Equation 23 to characterize the average effectiveness of LTES heat exchangers. Amin et al. [145] study a packed bed with spherical capsules of PCM. Since a single geometry was tested, the fitting coefficient *C* and the heat transfer surface area *A* are lumped in a single coefficient *CA*. The product *CA* is 0.0097 for solidification and 0.0112 for melting. López-Navarro et al. [146] tested a spiral coil in tank and correlated the effectiveness during melting and solidification with a constant of 0.0146 and 0.0168, respectively. Chen et al. [150] characterizes the averaged effectiveness of a finned tube LTES heat exchanger using Equation 23 with a value of 0.0256 for solidification and a value of 0.0168 for melting. Allouche et al. [148] compared a finned tube with active stirring to other designs in literature based on Equation 23. However, they did not report a value for the fitting constant *C* for their case.

In other cases, the value of the constant *C* proved to be a function of the mass flow rate. Tay et al. [158] developed a CFD model for the same shell and tube heat exchanger studied in [91, 159, 161]. The estimated effectiveness obtains good agreement with the experimental values for both melting and solidification cases. The average effectiveness as a function of mass flow rate drops as the flow in the HTF tubes transitions from turbulent to laminar. As a result, the average overall heat transfer coefficient which is associated with the value *C* is a function of the mass flow rate.

Most of the studies presented [91, 148, 150, 159, 161] focus on the effect of mass flow rate on the average effectiveness. According to the derivation of the effectiveness-NTU relation for LTES heat exchangers, the inlet temperature can influence the effectiveness by two effects. First, the temperature difference between the phase change temperature and inlet temperature is the driving potential for heat transfer. Second, the inlet temperature can influence the overall heat transfer coefficient either by influencing the HTF properties which can change the forced convection or by an increase of the temperature difference with the PCM which increases the Rayleigh number and thus possible natural convection in the PCM. The first effect is included in the definition of the effectiveness. The second effect is most often neglected and only one inlet temperature is tested.

The authors who do test multiple inlet temperature levels find contradicting results. López-Navarro et al. [146] tested three different inlet temperatures and found it to have a negligible influence on the averaged effectiveness. In contrast, Khan and Khan [97] found that the inlet temperature variation has a significant effect on the fitting factor *C*. The reason for this contrasting result might be found in the range of inlet temperatures tested. López-Navarro et al. [146] varied the inlet temperature within 4 °C and the driving temperature difference between 2 °C and 6 °C. Khan and Khan [97] on the other hand varied the inlet temperature and the driving temperature difference within respectively 15 °C and between 9.5 °C and 24.5 °C for melting and within 10 °C and between 27.5 °C and 37.5 °C.

Khan and Khan [97] takes the effect of the inlet temperature into account by defining the fitting coefficient *C* in Equation 23 as a function of the driving temperature difference (Equation 24). The fitting coefficients *a* and *b* have a value of 0.00072 and 0.0061 for melting and a value of 0.00052 and 0.0316 for solidification:

$$\bar{\varepsilon} = 1 - \exp\left(-\left(a\left(T_{in} - T_{pc}\right) + b\right)\frac{A}{\dot{m}}\right) \qquad 24$$

Increasing the driving temperature difference $|T_{in} - T_{pc}|$ increases the number of transfer units for melting. According to the effectiveness-NTU reasoning this can result from the inlet temperature affecting the convective heat transfer coefficient in the HTF or the temperature difference affecting the natural convection in the PCM. Khan and Khan [97] determine time averaged Rayleigh numbers and calculate Nusselt number predictions based on a correlation by Churchill and Chu [162] and find a significant variation in the Nusselt number. However, it is unclear whether this effect causes the change in fitting factor *C* since the effect of inlet temperature on the forced convection in the HTF is not investigated.

In contrast to the melting case, increasing the driving temperature difference $|T_{in} - T_{pc}|$ decreases the number of transfer units for solidification. This can probably not be attributed to natural convection as conduction is dominant during solidification in PCMs.

Besides the effect on the number of transfer units, the dependency of the fitting factor *C* on the inlet temperature might be a result of an increasing deviation of the charging cycle from the assumptions required to derive the effectiveness-NTU relation of Equation 18. In this derivation, the sensible heat of the PCM is neglected. However, the Stefan number ranges between 0.078 and 0.196 for the melting and 0.29 and 0.212 for the solidification indicating a significant portion of the internal energy change to be sensible.

It is not yet clear if the dependency of the average effectiveness on the temperature difference is a result of a change in NTU or in the ratio of sensible to latent heat. Therefore, further research is required on this topic.

One of the major benefits of the average effectiveness characterization by Equation 23 is the possibility of sizing heat exchangers since an increase in the tube length results in an increased heat transfer surface area. However, an increase in the surface area through the addition of fins is not well predicted by correspondingly increasing the fin surface area. Gil et al. [149] compared melting and solidification in a shell and tube heat exchanger, one with fins and one without fins. The non-finned designs found good agreement with the value for the constant *C* also found by [159]. The finned designs resulted in a significantly lower effectiveness compared for the same ratio of mass flow over heat transfer surface area, $\dot{m}/A$. However, the effectiveness of the finned designs is higher as a function of mass flow rate. The lower effectiveness as a function of the ratio $\dot{m}/A$ is thus caused by the lower effectiveness of fins compared to tube surface area.

In classic heat exchanger theory, fins are considered in the form of a fin surface efficiency. Amagour et al. [147] fitted a fin surface efficiency η_{fin} by adapting Equation 23 to Equation 25. Only a single value is tested, which results in a fin efficiency of 0.71:

$$\bar{\varepsilon} = 1 - \exp\left(-C\frac{(A_{unfinned} + \eta_{fin}A_{fin})}{\dot{m}}\right) \qquad 25$$

The studies discussed up to this point have fitted the effectiveness-NTU formulation of Equation 23 to experimental or numerical experiments. If the NTU can be predicted throughout the charging process, the averaged effectiveness can be found by averaging the right-hand side of Equation 18 in time. However, the NTU is better predicted as a function of the phase change fraction as is shown in literature [67, 142, 153, 156, 157].

To predict the averaged effectiveness, Tay et al. [161] averaged the effectiveness over the phase change fraction (Equation 26) instead of over the phase change time (Equation 21):

$$\bar{\varepsilon}_{\bar{\lambda}} = \int_0^1 \varepsilon_{pc}(\bar{\lambda})\, d\bar{\lambda} \qquad 26$$

To determine the averaged effectiveness using Equation 26, a relation between the instantaneous effectiveness ε_{pc} and the global liquid fraction $\bar{\lambda}$ is required. This relation is found by applying Equation 18 with the NTU related to the phase change fraction (Equation 27). The conditions for the effectiveness averaged over the liquid fraction $\bar{\varepsilon}_{\bar{\lambda}}$ to be equal to the effectiveness over time are discussed in Section 4. In the work of Tay et al. [161], the two averaged effectiveness are assumed equivalent.

$$\bar{\varepsilon}_{\bar{\lambda}} = \int_0^1 (1 - \exp(-NTU(\bar{\lambda}))\, d\bar{\lambda} \qquad 27$$

To determine the effectiveness averaged over the liquid fraction from Equation 27, the NTU must be described as a function of the phase change fraction. Therefore, a phase change front position as a function of the overall liquid fraction is assumed. The phase change front position results in a heat transfer resistance to the phase change front. This approach is similar to the approach followed by Belusko et al. [153] for estimating the instantaneous effectiveness. The predictions resulting from the method obtain reasonable agreement with the experimentally measured values. Belusko et al. [142, 157] used the same method to predict averaged effectiveness and compare it to the instantaneous effectiveness as a function of phase change fraction determined in a numerical study.

The model developed in [158] is used in [63] to simulate a different shell and tube heat exchanger. The effectiveness-NTU prediction developed in [161], is compared to experimentally found values and values found with CFD. The CFD obtains good agreement with the solidification experiments but not with the melting experiments since natural convection is neglected in the CFD. The effectiveness-NTU prediction underpredicts the average effectiveness however agrees reasonably well with the experimental values.

Table 2 summarizes the studies which use the effectiveness concept for LTES heat exchangers.

Table 2: Summary of papers on LTES heat exchangers using the effectiveness concept.

Parameter	Name	Predictive method	Coefficients	Year	Geometry	Source
ε_{ini}	Effectiveness based on initial temperature	-	-	2020	Finned tube	[124]
		-	-	2020	Module type	[103]
ε_{pc}	Effectiveness based on phase change temperature	Eq. 18	Analytical	1997	Tube in tube	[155]
		Eq. 18; Eq 19.	Experimental	1999	Planar	[138]
		Eq. 20	Analytical	2012	Planar	[153]
		Eq. 20	Experimental	2015	Direct contact	[156]
		Eq. 20	Numerical	2016	Shell and tube	[142, 157]
		Eq. 20	Experimental	2017	Shell and tube	[67]
$\bar{\varepsilon}$	Effectiveness averaged over time	Eq. 22	Polynomial	2011	Shell and tube	[91]
		Eq. 23	C=0.0199	2012	Shell and tube	[159]
		Eq. 23	CA=0097 & 0.0112	2012	Packed bed	[145]

		Eq. 23	-	2012	Shell and tube	[158]
		Eq. 23	C≈0.0199 (unfinned)	2013	Shell and tube	[149]
		Eq. 23	C=0.0146 & 0.0168	2014	Spiral coil	[146]
		Eq. 23	C=0.0168 & 0.0256	2014	Finned tube	[150]
		Eq. 23	-	2015	Finned tube	[148]
		Eq. 25	η_{fin}=0.71	2018	Shell and tube	[147]
		Eq. 24	C=0.1808 & 0.1991 a=0.00072 & 0.0061 b=0.00052 & 0.0316	2019	Shell and tube	[97]
$\bar{\varepsilon_{\bar{\lambda}}}$	Effectiveness averaged phase change fraction	Eq. 26	Analytical	2012	Tube in tube	[161]
		Eq. 26	Analytical	2012	Shell and tube	[63]

Heat transfer is often characterized in terms of Nusselt numbers or heat transfer coefficients. Therefore several authors use these concepts to characterize the heat transfer rate between HTF and PCM [64, 99] [69, 90, 103, 121, 148]. In the case of numerical studies, the heat transfer between HTF and container $\dot{Q}_{HTF-C}$ can be determined. In a numerical study on a shell and tube LTES heat exchanger, Khan et al. [99] defined the heat transfer coefficient in the PCM as Equation 28 and reported as a function of time.

$$K = \frac{\dot{Q}_{HTF-C}}{A\,(T_{in} - T_{pc})} \qquad 28$$

Khan et al. [99] express the heat transfer coefficient in a dimensionless Nusselt number and as a function of the Rayleigh number. Trp [64] takes a similar approach but determines a local Nusselt number along the flow length of the tubes. Lin et al. [121] determine the convective heat transfer coefficient as a function of the Reynolds number. These studies offer insight into the heat transfer processes, however they do not directly allow to estimate the efflux of energy since the internal energy change of the HTF is not characterized.

In experimental studies, directly measuring the heat transfer between the HTF and the container or PCM is not possible. Therefore, the heat transfer is determined by applying the conservation of energy to a control volume encompassing only the HTF (Equation 29):

$$\frac{dU_{HTF}}{dt} = \dot{F} + \dot{Q}_{HTF-C} \qquad 29$$

The heat transfer between HTF and container can be determined by measuring the efflux of energy $\dot{F}$ and estimating the change in internal energy of the HTF. However, very few authors estimate the energy stored in HTF as discussed in the section on state indicators. Therefore, most authors neglect the internal energy change of the HTF although it is not negligible at the start of a (dis)charging cycle [16, 62].

Jesumathy et al. [69] neglect the internal energy of the HTF and apply the logarithmic mean temperature difference ΔT_{LMTD} to define a heat transfer coefficient as in Equation 30. This approach is like the one Ismail et al. [138] used to define the NTU (Equation 19).

$$K = \frac{\dot{F}}{A\ \Delta T_{LMTD}} \quad (30)$$

The heat transfer coefficient was averaged in time and presented as a function of the HTF mass flow rate (Equation 28). Merlin et al. [90] and Reyes et al. [103] also average Equation 28 to determine a time averaged heat transfer coefficient.

$$\overline{K} = \frac{\bar{\dot{F}}}{A\ \overline{\Delta T}_{LMTD}} \quad (31)$$

If the overall heat transfer coefficient can be predicted, Equation 28 provides an additional method of estimating the average outlet temperature of the HTF besides the effectiveness-NTU approach. Allouche et al. [148] defined a Nusselt number based on the overall average heat transfer coefficient. The Nusselt number is correlated as a function of the Rayleigh number. However, the Nusselt number cannot be predicted from the correlation since the Rayleigh number is defined as a function of the bulk PCM temperature which has to measured.

3.2.2. Heat transfer over the boundary

In contrast to the efflux of energy, the heat transfer to the ambient is difficult to determine. To estimate it directly, the heat flux on the surface of the LTES heat exchanger should be measured and integrated in time and over the surface of the heat exchanger. To the knowledge of the authors, no study has attempted this. The heat transfer to the ambient however can be estimated based on an estimate of the internal energy change, efflux of energy and Equation 3 or 4 (e.g., [8], [90]). An alternative method for determining the heat loss is measuring the efflux of energy after the LTES system has reached steady state [118]. In most studies, the LTES heat exchanger is well insulated limiting losses to the ambient.

3.3. Time based indicators

Several time indicators can be defined. The difference between these indicators is the term in Equation 3 and 4 on which they are based. Two options are based on the internal energy change. First, time constants based on the total internal energy are referred to as charging time (e.g., [89, 93, 117, 124, 163-165]) and are defined by Equation 32. Second, time constants based on the latent heat (e.g., [46, 68, 69, 72, 77, 83, 87, 88, 90, 93, 96, 98, 99, 102, 104, 107-109, 113, 119, 120, 125, 129, 131-134, 136, 149, 165-170]) which are called melting/solidification time and are defined by Equation 33 with $\bar{\lambda}$ the total liquid fraction. A third type of time constant is based on the efflux of energy. These constants are defined by Equation 34 as the time required for the outlet temperature to reach a specific temperature level (e.g., [72, 76, 88, 90, 116, 118, 124, 148, 149]). Since time indicators are determined based on energy indicators or the efflux of energy, no additional measurements are required to determine time indicators.

$$t_c = t_x - t_{ini}\ for\ wich\ J(t_x) = J_{level} \quad (32)$$

$$t_{pc} = t_x - t_{ini}\ for\ which\ \bar{\lambda}(t_x) = \bar{\lambda}_{level} \quad (33)$$

$$t_T = t_x - t_{ini}\ for\ which\ T_{HTF}^{out}(t_x) = T_{level} \quad (34)$$

The three-time constants proposed by Equation 32-34 are based on a predefined level (J_{level}, $\bar{\lambda}_{level}$ and T_{level}). By altering this level, several time constants can be defined for a single experiment (e.g., [152]).

The phase change time defined by Equation 33 requires an accurate estimate of the total liquid fraction. As discussed above, obtaining an accurate estimate of the total liquid fraction is not an issue for numerical

studies and therefore it is often reported [65, 68, 77, 98, 99, 102, 104, 109, 120, 125, 129, 131-134, 136, 165]. In experimental studies, visual assessment of the phase change front is sometimes used (e.g., [83, 107]).

In case the liquid fraction level is chosen as one ($\bar{\lambda}_{level} = 1$ in Equation 33), a single local measurement at the location which changes phase last suffices for estimating the phase change time. For this method, a temperature sensor is most often used as a local liquid fraction sensor [69, 87, 88, 90, 93, 96, 108, 149].

Defining the charging time based on the outlet temperature of the HTF (Equation 34) is a common method in experimental studies since measuring the outlet temperature of the HTF is relatively accessible. Gasia et al. [164] defined the temperature level T_{level} based on the inlet temperature plus a fixed temperature difference. Other authors define the charging time based on a heat exchanger effectiveness. Moon et al. [124] defined a heat exchanger effectiveness based on the initial temperature of the storage. This effectiveness was used to define a charging time. Abokersh et al. [72] used Equation 34 with a temperature level of the minimum usable temperature in their application. Allouche et al. [148] defined the charging time as the time until the efflux of energy drops below 10 % of its initial value.

The charging time as defined by Equation 32 requires an estimate of the total stored energy. Since limited studies focus on the total stored energy [83, 89, 101, 137, 138], the definition is rarely used. In a numerical study, Kuboth et al. [165] used the definition with an energy level of 99.9 % of the maximum internal energy change. In experimental work, Martinelli et al. [89] and Beyne et al. [8, 152] applied the same definition. Martinelli et al. [89] applied the definition at 90 % of the maximum internal energy change. Beyne et al. [8] used 97.5 % in a first paper and varied the level between 1 and 99 % in a second paper [152].

Table 3 presents a summary of the reported time indicators and the papers which report them.

Table 3: Summary of the reported time indicators.

Parameter	Name	Numerical	Experimental
$t_c(J_{level})$	Charging time (function of stored energy)	[165]	[8, 89, 152]
$t_{pc}(\bar{\lambda}_{level})$	Phase change time	[65, 68, 77, 98, 99, 102, 104, 109, 120, 125, 129, 131-134, 136, 165]	[62, 69, 83, 87, 88, 90, 93, 96, 107, 108, 149]
$t_T(T_{level})$	Charging time (function of HTF outlet temperature)	-	[72, 124, 148, 164]

Several predictive models for time constants can be found in literature. The predictive models for time constants are based on an analytical solution for the phase change time of an LTES heat exchanger. This analytical solution was derived by Raud et al. [171] for a LTES heat exchanger with an overall heat transfer coefficient independent of the liquid fraction. The solution can be generalized (see Section 4.1.2.) as Equation 35 where t_0 is the time required for the phase change front to reach the edge of the heat exchanger at the inlet:

$$t_{pc}(\bar{\lambda}_{level} = 1) = t_0 + \frac{\Delta U}{\dot{m} c_p \Delta T_0} \quad 35$$

To determine t_0, an analytical solution of the Stefan problem was adapted by Bauer [172]. The predictions of Equation 35 were compared to CFD simulations for a shell and tube heat exchangers and found reasonable agreement.

Tarragona et al. [62] adapted the solution proposed by Raud et al. [171] for a planar geometry with a significant convective heat transfer resistance. The predictions obtained good agreement with experimentally measured phase change times.

In Equation 35, t_0 is the time required for the first cross section to change phase. In the simplified cases for which analytical solutions exist, t_0 is a function of the inverse of the temperature difference at the inlet. As a result, Equation 35 can be written as a function of the mass flow rate multiplied by the inverse of the temperature difference at the inlet. Beyne et al. [8] therefore proposed a correlation structure for both phase change time (Equation 33) and charging time (Equation 32). The correlation structure is given by Equation 36 with $f_s(\dot{m})$ and $f_i(\dot{m})$ two functions of the HTF mass flow rate:

$$\begin{cases} t_{pc}(\bar{\lambda}_{level} = 1) \\ \quad or \\ t_c(J_{level} = \Delta U) \end{cases} = f_s(\dot{m})\ \frac{1}{\Delta T_0} + f_i(\dot{m}) \qquad 36$$

Equation 36 includes a term which is not a function of the temperature difference between peak phase change temperature and PCM. This term is not a result from the derivation by Raud et al. [171]. However, this derivation requires several assumptions with amongst others neglecting all sensible heat. The term is thus required to adapt the correlation to conditions which deviate from the assumptions. Beyne et al. [8] collected several data sets with varying inlet temperatures but fixed mass flow rates and found good agreement with the correlation proposed in Equation 36.

Some data sets seem to deviate from Equation 36. Hosseini et al. [65] reported phase change time which do not seem to be hyperbolically related to the temperature difference at the inlet ΔT_0. Amin et al. [145] reported a time constant determined by a change in the gradient of the outlet temperature. Increasing mass flow rate and temperature difference resulted in an increased phase change time for some data points. As a result, Equation 36 was not applicable. Whether Equation 36 is applicable and under which assumptions thus requires further research.

Beyne et al. [8] performed an experimental campaign on the same heat exchanger as presented by Tarragona et al. [62]. The slope function $f_s(\dot{m})$ was based on the work of Raud et al. [171] while the best fitting function with two variables was chosen for the intercept function $f_i(\dot{m})$. The resulting correlation is shown in Equation 37 with a, b, c, and d fitting coefficients:

$$t_c = \left(a + \frac{b}{\dot{m}}\right) \frac{1}{\Delta T_0} + c e^{d\,\dot{m}} \qquad 37$$

The definition for the charging time is linked to a change in internal energy of the LTES heat exchanger. As such it can be expanded to predict the internal energy change as a function of time and the outlet temperature for given inlet conditions. This expansion is called the charging time energy fraction model and was presented by Beyne et al. [152].

The charging time energy fraction method first estimates the total energy change of a LTES heat exchanger undergoing a temperature change between the initial temperature T_{ini} and the inlet temperature T_{in}. This

internal energy change ΔU is given by Equation 38 and is a function of initial and inlet conditions and material properties which are assumed to be known:

$$\Delta U(T_{ini}, T_{in}) = m_{HTF}\left(u_{HTF}(T_{in}) - u_{HTF}(T_{ini})\right) + m_C\left(u_C(T_{in}) - u_C(T_{ini})\right) + m_{PCM}\left(u_{PCM}(T_{in}) - u_{PCM}(T_{ini})\right) \quad 38$$

The internal energy change is used to define an energy fraction (Equation 39) which provides a relative expression for the change of internal energy of the LTES heat exchanger:

$$\alpha = \frac{J(t)}{\Delta U(T_{ini}, T_{in})} \quad 39$$

The charging time is related to the energy fraction through the definition expressed by Equation 32. It is correlated for a series of energy fractions using Equation 40, an adaptation of the correlation used in [8] to obtain a better fit at lower energy fractions. Equation 40 is correlated for energy fractions between 0.01 and 0.99 resulting in a list of fitting parameters *a*, *b*, *c,* and *d* as a function of the energy fraction α:

$$t_c(\alpha) = \left(a(\alpha) + \frac{b(\alpha)}{\dot{m}}\right)\frac{1}{\Delta T_0} + \left(c(\alpha) + \frac{d(\alpha)}{\dot{m}}\right) \quad 40$$

By associating a time to a set of energy fractions, the stored energy as a function of time can be predicted. Since the heat transfer to the ambient is neglected, the stored energy is equal to the integrated efflux of energy (see Equation 3). By deriving the integrated efflux of energy with respect to time, the outlet temperature of the HTF can be estimated.

The charging time energy fraction method provides a tool to predict the outlet temperature of LTES heat exchangers as a function of time. The method is thus more general than the averaged effectiveness method or phase change time method since both averaged effectiveness and charging time can be predicted using the coefficient of a charging time energy fraction model. However, there is no method available to quantitively link the fitting coefficients of the model to the geometry and material properties of the LTES systems. The model thus requires a set of experiments to fit these coefficients. It is therefore useful for characterizing the LTES heat exchanger, but not for design or sizing.

4. Predictive models for process performance indicators

To characterize a LTES heat exchanger, the performance indicators must be predictable for a given operational point. The operational point is defined by the ingoing HTF mass flow rate and state as well as the ambient temperature. A predictive model as described above thus has the structure as shown in Figure 4. Determining a predictive model for an LTES heat exchanger will be called characterizing the LTES heat exchanger.

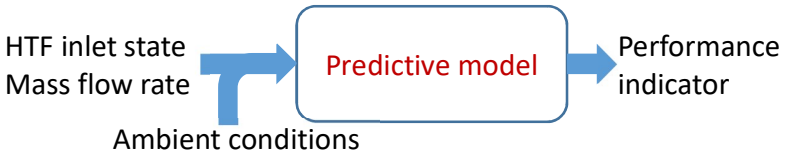

Figure 4: Schematic representation of a predictive model for LTES heat exchanger performance indicators.

The coefficients of the predictive model are either determined by fitting to (numerical) experiments or estimated based on geometry and material parameters. If the parameters are a function of geometric parameters, the predictive model can be used to design LTES heat exchangers. Therefore, these models will be referred to as design models.

An example of a fitted model is the model resulting from the charging time energy fraction method. The predictive model allows to estimate the performance of an LTES heat exchanger in a specific application. However, it does not allow estimating the performance of an LTES heat exchanger with a change in PCM properties or geometry.

The phase change time models of Raud et al. [171] and Tarragona et al. [62] and averaged effectiveness estimations of Tay et al. [63, 161] are examples of design models. The phase change time or averaged effectiveness is estimated as a function of material and geometric parameters. The effect of the change of each of these parameters can be determined.

The fitted averaged effectiveness correlations according to Equation 22, 20 and 20 are design models for the heat transfer surface area. The effect of varying other geometric or material parameters cannot necessarily be estimated.

The design models found for LTES heat exchangers are thus based on two approaches: the effectiveness-NTU approach and the phase change time approach. In the current section the theoretical background of the approaches is investigated and both approaches are compared.

4.1. Derivation of effectiveness-NTU relation and phase change time relation

The derivation of the effectiveness-NTU relation and phase change time is based on a similar set of assumptions. The HTF is represented as being at the bulk temperature in the entire cross section. The bulk temperature of the HTF only varies along the flow length which is placed along the bulk flow direction of the HTF (this direction will be designated as the x-axis). The internal energy change of the heat transfer fluid and container and the sensible energy change of the PCM are neglected. Heat transfer in the direction of the flow in the PCM is neglected and the specific heat capacity of the HTF is assumed constant.

The effectiveness-NTU derivation is based on the conservation of energy applied to the HTF while the phase change time derivation is based on the conservation of energy applied to the entire LTES heat exchanger.

4.1.1. Effectiveness-NTU

By neglecting diffusive transport with respect to convective transport in the HTF, the conservation of energy for an infinitesimal control volume of HTF is expressed by Equation 41:

$$\frac{d(dU_{HTF})}{dt} = \dot{m} c_p dT + d\dot{Q}_{PCM-HTF} \qquad 41$$

Figure 5 shows a schematic representation of the heat exchanger and the infinitesimal control volume on which Equation 41 is applied.

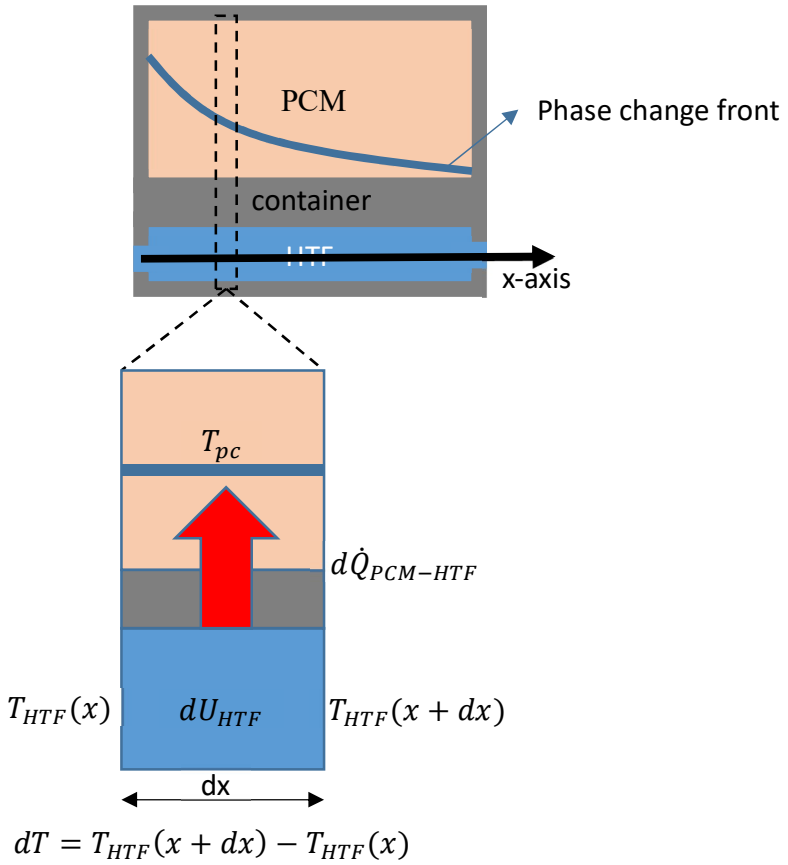

Figure 5: Infinitesimal section of a LTES heat exchanger used for expressing Equation 41.

In steady-state analysis of heat exchangers, the internal energy change of the HTF $\frac{dU_{HTF}}{dt}$ can be neglected. LTES heat exchangers do not operate in steady state, however the internal energy change of the HTF can be neglected compared to the internal energy change of the PCM. This assumption is also sometimes used for the dynamic simulation of heat exchangers (e.g., [173]). As a result, Equation 41 reduces to Equation 42:

$$0 = \dot{m} c_p dT + d\dot{Q}_{PCM-HTF} \qquad 42$$

By neglecting the sensible heat capacity of the PCM and container, the heat transfer over the edge of the HTF control volume $d\dot{Q}_{PCM-HTF}$ is equal to the heat transfer between the HTF and the phase change front. Furthermore, assuming an isothermal phase change allows writing the heat transfer as a function of the temperature difference between the local HTF bulk temperature and the PCM.

The heat transfer between PCM and HTF is written in terms of a local heat transfer coefficient per unit length $KP(x,t)$ (Equation 43):

$$d\dot{Q}_{PCM-HTF} = KP(x,t)\,dx\,(T_{pc} - T_{HTF}(x,t)) \quad 43$$

Note that at this point the derivation between the classic effectiveness method for steady state heat exchangers deviates from what is presented here. Due to the movement of the phase change front, the local heat transfer coefficient per unit length *KP(x,t)* is a function of both position and time while in classic, steady-state heat exchangers it is only a function of position. This corresponds to the effectiveness and outlet temperature of LTES heat exchangers being functions of time.

Substituting Equation 43 in Equation 42 and rearranging results in Equation 44:

$$\frac{dT_{HTF}}{dx} = \frac{KP(x,t)}{\dot{m}c_p}(T_{pc} - T_{HTF}(x,t)) \quad 44$$

Equation 44 can be solved by separating the temperature and position variables. The local heat transfer coefficient per unit length KP can be a function of both temperature and position. The local heat transfer coefficient should be written as the product of a function of the position and a function of the temperature similar as is done for steady-state heat exchangers [174]. In the present discussion, the effect of temperature will be neglected as neglecting the temperature effect will result in the effectiveness expressed by the commonly used Equation 18. Separating the variables in Equation 44 thus results in Equation 45:

$$\frac{d(T_{HTF})}{(T_{pc} - T_{HTF})} = \frac{KP(x,t)}{\dot{m}c_p}dx \quad 45$$

The phase change temperature is a constant which allows rewriting the differential on the left-hand side of Equation 45 as Equation 46:

$$d(T_{HTF}) = -d(T_{pc} - T_{HTF}) \quad 46$$

Substituting Equation 45 into Equation 46 and integrating both sides of the equation results in Equation 47 with the overall heat transfer coefficient *KA* defined by Equation 48 and the temperature boundary conditions defined in Equation 49:

$$ln\left(\frac{T_{pc} - T_{out}(t)}{T_{pc} - T_{in}}\right) = -\frac{KA(t)}{\dot{m}c_p} \quad 47$$

$$with\ KA(t) = \int_0^L KP(x,t)dx \quad 48$$

$$with\ T_{HTF}(x=0) = T_{in}\ \&\ T_{HTF}(x=L) = T_{out} \quad 49$$

By applying the inlet condition expressed by Equation 49, the effectiveness of the heat exchanger can be written as Equation 50 with the number of transfer units (NTU) defined by Equation 51:

$$\varepsilon_{pc}(t) = \frac{T_{out}(t) - T_{in}}{T_{pc} - T_{in}} = 1 - \exp\left(-\frac{KA(t)}{\dot{m}c_p}\right) \quad 50$$

$$NTU(t) = \frac{KA(t)}{\dot{m}c_p} \quad 51$$

Under the assumption of negligible energy except for the latent heat, the effectiveness as defined by Equation 50 corresponds to the ratio of the heat transfer rate to the maximum possible heat transfer rate. Besides the time dependency of the relation, the relation between effectiveness and NTU is the same as

for steady-state heat exchangers with one fluid at a constant temperature (see e.g. [47]). However, the required assumptions to derive Equation 50 are specific to the case of LTES heat exchangers.

Most authors do not use the instantaneous effectiveness, but they define and correlate a time averaged effectiveness (see Equation 21).

$$\bar{\varepsilon} = \frac{1}{t_2 - t_1} \int_{t_1}^{t_2} \varepsilon_{pc}(t)\, dt \qquad \text{Eq. 21}$$

To solve the integral in Equation 21, an expression of the NTU as a function of time is required. However, it is easier to determine an expression of the NTU as a function of the position of the phase change front or the phase change fraction. Therefore, several authors determine the effectiveness averaged over phase change fraction (see Equation 26).

$$\bar{\varepsilon}_{\bar{\lambda}} = \int_0^1 \varepsilon_{pc}(\bar{\lambda})\, d\bar{\lambda} \qquad \text{Eq. 26}$$

The relation between the effectiveness averaged over time $\bar{\varepsilon}$ (Equation 21) and averaged over phase change fraction $\bar{\varepsilon}_{\bar{\lambda}}$ (Equation 26) can be found by changing the integration variable in the integral of Equation 21 (Equation 52). For both definitions to be equivalent, the derivative of time to the overall liquid fraction $\frac{dt}{d\bar{\lambda}}$ should be equal to the phase change time $t_2 - t_1$. This implies a constant heat transfer rate during phase change since time and overall liquid fraction are linearly related. This is the case if the heat transfer resistance in the PCM is negligible compared to the heat transfer resistance of container and HTF.

$$\bar{\varepsilon} = \frac{1}{t_2 - t_1} \int_{t_1}^{t_2} \varepsilon_{pc}(t)\, dt = \frac{1}{t_2 - t_1} \int_0^1 \varepsilon_{pc}(\bar{\lambda}) \frac{dt}{d\bar{\lambda}} d\bar{\lambda} \qquad 52$$

An alternative can be found to the restriction of a constant heat transfer rate by expressing that heat transfer between HTF and PCM results in a change of liquid fraction (Equation 53):

$$\frac{d\bar{\lambda}}{dt} = \frac{\dot{m} c_p \Delta T_0}{\Delta U} (1 - \exp(NTU(\bar{\lambda})) \qquad 53$$

Equation 53 is an ordinary differential equation which can be resolved numerically. The time averaged liquid fraction is found by Equation 54 with $t_{\bar{\lambda}=1}$ the time where the liquid fraction reaches one. The procedure outlined in Equation 53 and 54 does not require additional assumptions however no author in literature uses this approach.

$$\bar{\varepsilon} = \frac{J}{\dot{m} c_p \Delta T_0\, t_{\bar{\lambda}=1}} \qquad 54$$

4.1.2. Phase change time

The conservation of energy is expressed on the LTES heat exchanger by Equation 3. By neglecting the heat loss to the environment and assuming a constant specific heat of the HTF, Equation 3 reduces to Equation 55:

$$\frac{dU}{dt} = \dot{m}\, c_p (\, T_{in} - T_{out}) \qquad 55$$

The phase change temperature is introduced in Equation 55 by expressing the temperature difference between inlet and outlet of the HTF as a function of the temperature difference between the phase change front and the HTF. The temperature difference at the inlet ΔT_0 and at the outlet ΔT_L is given by respectively Equation 56 and 57:

$$\Delta T_0 = T_{in} - T_{pc} \quad 56$$

$$\Delta T_L = T_{out} - T_{pc} \quad 57$$

Equation 55 can be rewritten as a function of the temperature differences defined in Equation 56 and 57:

$$\frac{dU}{dt} = \dot{m}\, c_p(\Delta T_0 - \Delta T_L) \quad 58$$

The temperature at the inlet and the mass flow rate of the HTF are constant inlet conditions. The temperature at the outlet is a function of time. Therefore, an averaged outlet temperature difference is defined by Equation 59 with t_L the phase change time:

$$\Delta \bar{T}_L = \frac{1}{t_L}\int_0^{t_L} \Delta T_L\, dt \quad 59$$

Equation 58 is integrated in time which results in Equation 60:

$$J = \dot{m}\, c_p(\Delta T_0 t_L - \Delta \bar{T}_L t_L) \quad 60$$

Equation 60 has two remaining unknown variables: t_L and $\Delta \bar{T}_L$. Characterizations of phase change problems under constant boundary conditions are reviewed to find a relation between the phase change time and average temperature difference at the outlet. These constant boundary condition characterizations provide a correlation between three variables: the phase change fraction λ_A, the time t and the driving temperature difference ΔT which is constant as a function of time. The correlation between the three variables can be expressed as Equation 61:

$$\lambda_A = f(t, \Delta T) \quad 61$$

Equation 61 is valid for a constant temperature difference. However, this is only the case at the inlet of the LTES heat exchanger. In the present derivation, the relation given by Equation 61 is assumed to hold for a varying inlet temperature by replacing the time dependent temperature difference with the time averaged temperature difference (Equation 62 and Equation 63):

$$\lambda_A = f(t, \Delta \bar{T}) \quad 62$$

$$with\ \Delta \bar{T} = \frac{1}{t}\int_0^{t} \Delta T\, dt \quad 63$$

Equation 62 is only true under specific conditions. To obtain the required conditions, the heat transfer between PCM and HTF is written as the resulting change of the internal energy of the PCM. Since the sensible heat of the PCM is neglected, applying the conservation of energy to an infinitesimally short control volume of PCM (see Figure 5) results in Equation 64 with ΔU_A the internal energy per unit length

and λ_A the liquid fraction averaged over the surface area as defined by respectively Equation 65 and Equation 66:

$$d\dot{Q}_{PCM-HTF} = \Delta U_A \frac{d\lambda_A}{dt}\, dx \quad (64)$$

$$\Delta U_A = \iint \rho_{PCM}\, h_{lat}\, dy\, dz \quad (65)$$

$$\lambda_A = \frac{1}{A} \iint \lambda(x,y,z)\, dy\, dz \quad (66)$$

The heat transfer from PCM to HTF is modelled as the product of an overall heat transfer coefficient per unit length KP and the temperature difference ΔT. Substituting this product in Equation 64 results in Equation 67:

$$KP\, \Delta T = \Delta U_A \frac{d\lambda_A}{dt} \quad (67)$$

The expression for the surface averaged liquid fraction λ_A is found by separating the variables in Equation 68:

$$\Delta T\, dt = \frac{\Delta U_A}{KP} d\lambda_A \quad (68)$$

If the overall heat transfer coefficient can be written as a function of only the liquid fraction, Equation 65 can be integrated to obtain Equation 69:

$$\Delta \bar{T}\, t = \int \frac{\Delta U_A}{KP} d\lambda_A \quad (69)$$

For Equation 62 to be applicable, the overall heat transfer coefficient must be expressible as a function of only the liquid fraction (Equation 70). Otherwise, separating the variables in Equation 68 is not valid.

$$KP = \frac{\Delta U_A}{\Delta T} \frac{d\lambda_A}{dt} \; can\ be\ written\ as\ a\ function\ of\ only\ \lambda_A \quad (70)$$

The second condition for Equation 59 to be applicable is that the integral in Equation 67 can be determined and solved resulting in the form of Equation 59 (Equation 71):

$$\Delta \bar{T}\, t = \int \frac{\Delta T}{\frac{d\lambda_A}{dt}} d\lambda_A \; can\ be\ solved\ for\ \lambda_A\ in\ the\ form\ of\ Equation\ 62 \quad (71)$$

Equations 70 and 71 pose two conditions on the function $f(t, \Delta T)$ for Equation 62 to be valid.

Equation 69 can be rearranged to show that the time required to reach a specific liquid fraction is inversely related to the temperature difference (Equation 72):

$$t \sim \frac{1}{\Delta T} \quad (72)$$

The phase change time t_L and average temperature difference at the heat exchanger outlet $\Delta \bar{T}_L$ can thus be related as a function of the temperature difference at the inlet and the time required for complete phase change at the inlet t_0 (Equation 73):

$$\Delta\bar{T}_L = \frac{\Delta T_0 t_0}{t_L} \quad (73)$$

Equation 72 is substituted in Equation 60 which results in Equation 74:

$$J = \dot{m}\, c_p(\, \Delta T_0 t_L - \Delta T_0 t_0) \quad (74)$$

Equation 74 can be solved for the phase change time (Equation 75):

$$t_L = t_{pc} = t_0 + \frac{J}{\dot{m}\, c_p \Delta T_0} \quad (75)$$

4.2. Comparison of the models

The assumptions required to derive the melting time, the instantaneous effectiveness-NTU and the averaged effectiveness NTU method are listed in

Table 4. The first 8 assumptions are required for all three of the models. The eighth assumption is required for the instantaneous effectiveness to be estimated by Equation 50. The ninth assumption is required for the time averaged effectiveness and liquid fraction averaged effectiveness to be equal. It is not required if the time averaged liquid fraction is determined using the ordinary differential equation outlined in Equation 53.

Table 4: Required assumptions for the derivation of predictive models.

$\varepsilon(NTU)$	$\bar{\varepsilon} = \bar{\varepsilon}_{\bar{\lambda}}$	t_{pc}
1. No conduction in the flow direction in PCM, HTF or container. 2. No internal energy change of the HTF. 3. HTF at bulk temperature. 4. HTF properties independent of temperature. 5. No sensible heat capacity in the PCM and container. 6. Isothermal phase change. 7. No heat losses to the ambient. 8. The local heat transfer coefficient per unit length is not a function of temperature.		
	9. The local heat transfer coefficient per unit length is constant in time.	10. Equation 69.

Both derivations are linked by expressing the average effectiveness as a function of the phase change time (Equation 76):

$$\bar{\varepsilon} = \frac{J}{\dot{m} c_p \Delta T_0 t_{pc}} \quad (76)$$

Substituting Equation 74 into Equation 76 gives an alternative expression for the averaged effectiveness (Equation 77). The factor $\frac{c_p \Delta T_0 t_0 P}{\Delta U_A}$ is not a function of mass flow rate if the convective heat transfer coefficient of the HTF does not strongly vary with mass flow rate, therefore Equation 74 can be fitted for a fixed inlet temperature.

$$\bar{\varepsilon} = \frac{1}{\frac{\dot{m}}{A}\frac{c_p \Delta T_0 t_0 P}{\Delta U_A} + 1} \quad (77)$$

Equation 77 can be used as an alternative to Equation 23 for fitting time averaged effectiveness data. The studies in Table 2 report fitting coefficients between 0.01 and 0.2 with a mass flow rate over heat transfer surface area between 0.02 and 0.45 kg/(s m²). In this range, Equation 77 can be fitted with a root mean square deviation below 5 %. Equation 77 and 23 are thus similar for fitting data in the ranges found in literature.

Two studies have been found which report both phase change time and averaged effectiveness. The time constant reported by Amin et al. [145] is based on a change in gradient in the outlet temperature. Due to this qualitative definition, the reported time constant does not coincide with the phase change time and effectiveness and time constants are not related through Equation 76. The time constants reported by Gil et al. [149] are phase change times and the total stored latent energy is also given. In Figure 6, the effectiveness calculated using Equation 76 is compared to the measured effectiveness. The effectiveness based on Equation 76 is an overestimation, however the calculation shows the correct trend.

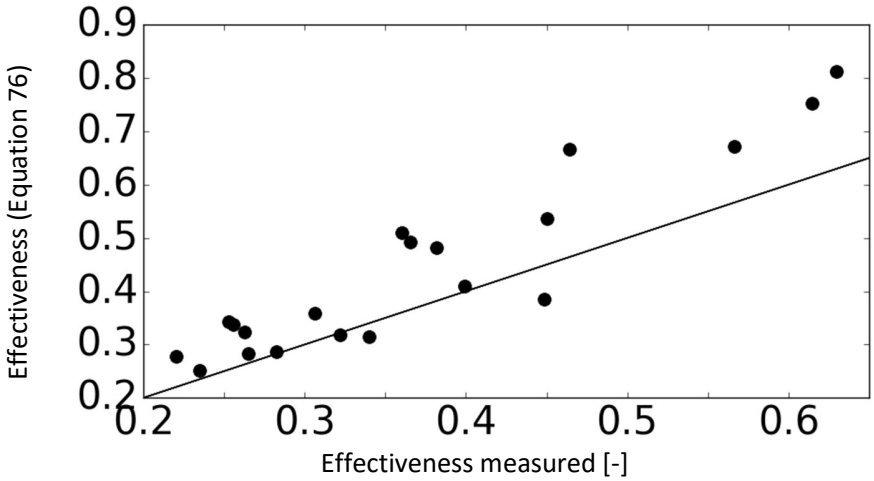

Figure 6: The effectiveness measured and calculated from phase change time data. Based on data reported in the work of Gil et al. [149].

A third dataset to which the authors of this paper have access is the one presented by Tarragona et al. [62]. The measured effectiveness during the phase change time is compared to the estimated effectiveness based on the predictive model for phase change time presented in Tarragona et al. [62] and Equation 76.

Figure 7 shows the effectiveness predictions as a function of the measured effectiveness when only taking the latent heat into account. The data is split into three levels with an effectiveness around 0.2, 0.3, and 0.4. These groups correspond to three mass flow rates. The model obtains similar predictions since the effectiveness is not a function of the temperature difference according to Equation 76 if the phase change time at the inlet t_0 is inversely related to the temperature difference.

Figure 8 shows the same predicted effectiveness as a function of measured effectiveness with a difference in the estimation of the total internal energy change J. In Figure 7 only the latent heat of the PCM is considered while in Figure 8 both latent and sensible heat of PCM and container material are taken into account. As can be seen by comparing Figure 7 and Figure 8, considering the sensible heat results in a higher accuracy of the prediction. However, considering sensible heat is a deviation from the assumptions required for both the effectiveness-NTU and phase change time derivations.

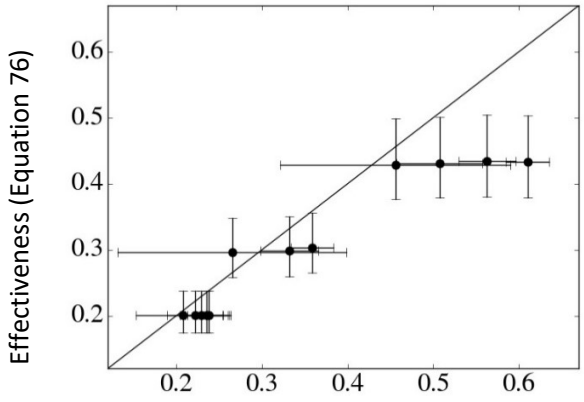

Figure 7: The effectiveness predicted from the phase change time predictive method as a function of the measured effectiveness taking only the latent heat into account. Based on the data from the work of Tarragona et al. [62].

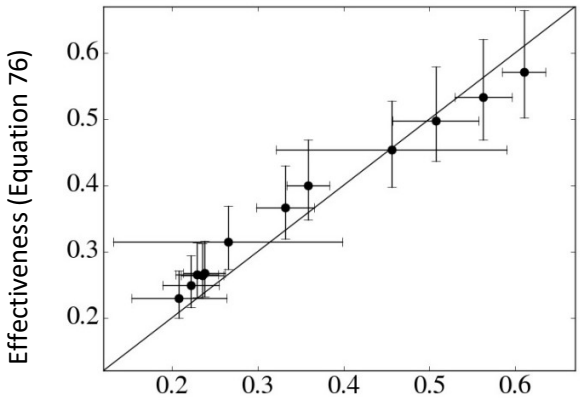

Figure 8: The effectiveness predicted from the phase change time predictive method as a function of the measured effectiveness taking both latent and sensible heat into account. Based on the data from the work of Tarragona et al. [62].

The results presented in Figure 8 show that the sensible heat should be considered when correlating the averaged effectiveness. However, the sensible heat is neglected in the derivation of both the effectiveness-NTU and the phase change time method. As a result, Equation 76 does not result in an accurate translation between averaged effectiveness and phase change time for experimental data. Therefore, we recommend to characterize two out of the three indicators in Equation 76: effectiveness, phase change time and/or change in internal energy.

Equation 32 presents a charging time definition which links time constants to total internal energy change rather than only the latent energy change. The charging time energy fraction method uses this definition to characterize the outlet temperature and internal energy change of a LTES heat exchanger [175]. However, the model includes multiple energy fractions between 0 and 1. Since the two design methods presented in Section 4.1 are exclusively for a phase change fraction of 1, the charging time energy fraction method currently cannot be used for designing LTES heat exchangers but only to characterize LTES heat exchangers.

A second recommendation for further work is therefore finding an analytic solution of the problem posed in Section 4.1.2. for phase change fractions between 0 and 1. If such a solution is known, the coefficients of the charging time energy fraction method might be predicted or interpreted physically.

A final recommendation results from reviewing the assumptions presented in

Table 4 and the assumptions used in the charging time energy fraction method. The heat transfer to the environment is neglected in both the effectiveness-NTU, phase change time and charging time energy fraction method. However, the heat losses will not always be negligible. Therefore, we recommend investigating the effect of heat transfer to the ambient on effectiveness, phase change time and charging time energy fraction models.

5. Conclusions

LTES heat exchangers are a well-studied topic in literature. However, comparing results from different studies on LTES heat exchangers remains difficult due to the different performance indicators reported for LTES system operation. This is the result of a lack of a standardized thermodynamic framework for studying LTES heat exchangers.

In the present paper, a thermodynamic framework is presented for LTES heat exchangers and their performance indicators. Based on the framework, technical performance indicators are categorized in three major groups: state indicators, energy transfer indicators and time indicators. The energy transfer indicators and to a lesser extent the time indicators are identified as candidates for key performance indicators. Based on an extensive literature review which focusses on reported indicators, predictive models are found for three possible key performance indicators: averaged effectiveness, phase change time and charging time. The averaged effectiveness and phase change temperature are related through the thermodynamic framework. However, the relation between averaged effectiveness and phase change time requires further investigation due to the deviations from the assumptions made during the derivation of the characterization models. We recommend to characterize both averaged effectiveness and phase change time in future works.

The charging time energy fraction method is a promising method to characterize charging time, internal energy change and outlet temperature as a function of time. However, there is no clear physical interpretation of its coefficients due to a lack of a theoretical solution for charging time. Furthermore, the method should be tested for more geometries and operating conditions before it can be seen as a generally applicable model for LTES heat exchangers.

A final recommendation follows from the assumptions of the theoretical models and the charging time energy fraction model. All these methods neglect heat transfer between the LTES heat exchanger and the ambient. However, this is not necessarily valid. Therefore, the effect of heat transfer to the ambient needs further investigation.

Acknowledgements

This work was partially funded by the Ministerio de Ciencia, Innovación y Universidades de España (RTI2018-093849-B-C31 - MCIU/AEI/FEDER, UE) and by the Ministerio de Ciencia, Innovación y Universidades - Agencia Estatal de Investigación (AEI) (RED2018-102431-T). Dr. Cabeza would like to thank the Catalan Government for the quality accreditation given to her research group GREiA (2017 SGR 1537). GREiA is a certified agent TECNIO in the category of technology developers from the Government of Catalonia. This work is partially supported by ICREA under the ICREA Academia programme.

This research was supported by Flanders Make, the strategic research centre for the manufacturing industry, Belgium.

References

[1] K. Faraj, M. Khaled, J. Faraj, F. Hachem, and C. Castelain, "Phase change material thermal energy storage systems for cooling applications in buildings: A review," *Renewable and Sustainable Energy Reviews,* vol. 119, p. 109579, 2020.

[2] Y. K. Zhou *et al.*, "Passive and active phase change materials integrated building energy systems with advanced machine-learning based climate-adaptive designs, intelligent operations, uncertainty-based analysis and optimisations: A state-of-the-art review," *Renew. Sust. Energ. Rev.,* vol. 130, Sep 2020, Art no. 109889, doi: 10.1016/j.rser.2020.109889.

[3] R. Zeinelabdein, S. Omer, and G. Gan, "Critical review of latent heat storage systems for free cooling in buildings," *Renew. Sust. Energ. Rev.,* vol. 82, pp. 2843-2868, Feb 2018, doi: 10.1016/j.rser.2017.10.046.

[4] J. Lizana, R. Chacartegui, A. Barrios-Padura, and C. Ortiz, "Advanced low-carbon energy measures based on thermal energy storage in buildings: A review," *Renew. Sust. Energ. Rev.,* vol. 82, pp. 3705-3749, Feb 2018, doi: 10.1016/j.rser.2017.10.093.

[5] C. A. Ikutegbe and M. M. Farid, "Application of phase change material foam composites in the built environment: A critical review," *Renew. Sust. Energ. Rev.,* vol. 131, Oct 2020, Art no. 110008, doi: 10.1016/j.rser.2020.110008.

[6] I. R. Segundo, E. Freitas, V. Branco, S. Landi, M. F. Costa, and J. O. Carneiro, "Review and analysis of advances in functionalized, smart, and multifunctional asphalt mixtures," *Renew. Sust. Energ. Rev.,* vol. 151, Nov 2021, Art no. 111552, doi: 10.1016/j.rser.2021.111552.

[7] B. Lamrani, K. Johannes, and F. Kuznik, "Phase change materials integrated into building walls: An updated review," *Renew. Sust. Energ. Rev.,* vol. 140, Apr 2021, Art no. 110751, doi: 10.1016/j.rser.2021.110751.

[8] W. Beyne, K. Couvreur, S. Lecompte, and M. De Paepe, "A technical, financial and CO2 emission analysis of the implementation of metal foam in a thermal battery for cold chain transport," *Journal of Energy Storage,* vol. 35, p. 102324, 2021/03/01/ 2021, doi: https://doi.org/10.1016/j.est.2021.102324.

[9] Y. Zhao, X. Zhang, and X. Xu, "Application and research progress of cold storage technology in cold chain transportation and distribution," *Journal of Thermal Analysis and Calorimetry,* vol. 139, no. 2, pp. 1419-1434, 2020/01/01 2020, doi: 10.1007/s10973-019-08400-8.

[10] M. K. A. Sharif *et al.*, "Review of the application of phase change material for heating and domestic hot water systems," *Renewable and Sustainable Energy Reviews,* vol. 42, pp. 557-568, 2015/02/01/ 2015, doi: https://doi.org/10.1016/j.rser.2014.09.034.

[11] P. D. Lund, J. Lindgren, J. Mikkola, and J. Salpakari, "Review of energy system flexibility measures to enable high levels of variable renewable electricity," *Renewable and sustainable energy reviews,* vol. 45, pp. 785-807, 2015.

[12] A. Palacios, C. Barreneche, M. Navarro, and Y. Ding, "Thermal energy storage technologies for concentrated solar power–A review from a materials perspective," *Renewable Energy,* 2019.

[13] G. A. Farulla, M. Cellura, F. Guarino, and M. Ferraro, "A Review of Thermochemical Energy Storage Systems for Power Grid Support," *Applied Sciences,* vol. 10, no. 9, p. 3142, 2020.

[14] R. Khatri, R. Goyal, and R. K. Sharma, "Advances in the developments of solar cooker for sustainable development: A comprehensive review," *Renew. Sust. Energ. Rev.,* vol. 145, Jul 2021, Art no. 111166, doi: 10.1016/j.rser.2021.111166.

[15] A. K. Pandey, M. S. Hossain, V. V. Tyagi, N. Abd Rahim, J. A. L. Selvaraj, and A. Sari, "Novel approaches and recent developments on potential applications of phase change materials in solar energy," *Renew. Sust. Energ. Rev.,* vol. 82, pp. 281-323, Feb 2018, doi: 10.1016/j.rser.2017.09.043.

[16] A. Castell and C. Solé, "Design of latent heat storage systems using phase change materials (PCMs)," in *Advances in Thermal Energy Storage Systems*: Elsevier, 2015, pp. 285-305.

[17] M. M. Kenisarin, "High-temperature phase change materials for thermal energy storage," *Renewable and sustainable energy reviews,* vol. 14, no. 3, pp. 955-970, 2010.

[18] M. Kenisarin and K. Mahkamov, "Salt hydrates as latent heat storage materials:Thermophysical properties and costs," *Solar Energy Materials and Solar Cells,* vol. 145, pp. 255-286, 2016/02/01/ 2016, doi: https://doi.org/10.1016/j.solmat.2015.10.029.

[19] S. C. Costa and M. Kenisarin, "A review of metallic materials for latent heat thermal energy storage: Thermophysical properties, applications, and challenges," *Renew. Sust. Energ. Rev.,* vol. 154, Feb 2022, Art no. 111812, doi: 10.1016/j.rser.2021.111812.

[20] G. S. Wei *et al.*, "Selection principles and thermophysical properties of high temperature phase change materials for thermal energy storage: A review," *Renew. Sust. Energ. Rev.,* vol. 81, pp. 1771-1786, Jan 2018, doi: 10.1016/j.rser.2017.05.271.

[21] Rubitherm. "Organic PCM - RT." https://www.rubitherm.eu/en/index.php/productcategory/organische-pcm-rt (accessed 24/01, 2017).

[22] L. F. Cabeza, A. Castell, C. Barreneche, A. de Gracia, and A. I. Fernández, "Materials used as PCM in thermal energy storage in buildings: A review," *Renewable and Sustainable Energy Reviews,* vol. 15, no. 3, pp. 1675-1695, 2011/04/01/ 2011, doi: https://doi.org/10.1016/j.rser.2010.11.018.

[23] J. Lizana, R. Chacartegui, A. Barrios-Padura, and J. M. Valverde, "Advances in thermal energy storage materials and their applications towards zero energy buildings: A critical review," *Appl. Energy,* vol. 203, pp. 219-239, 2017/10/01/ 2017, doi: https://doi.org/10.1016/j.apenergy.2017.06.008.

[24] L. F. Cabeza, Mehling, M., *Heat and cold storage with PCM: An up to date introduction into basics and applications*. Springer-Verlag Berlin Heidelberg, 2008.

[25] M. M. Farid, A. M. Auckaili, and G. Gholambozanjani, Eds. *Thermal energy storage with phase change materials*, First edition ed. Boca Raton: CRC Press, Taylor & Francis Group, 2021, p. 1.

[26] B. J. Nie, A. Palacios, B. Y. Zou, J. X. Liu, T. T. Zhang, and Y. R. Li, "Review on phase change materials for cold thermal energy storage applications," *Renew. Sust. Energ. Rev.,* vol. 134, Dec 2020, Art no. 110340, doi: 10.1016/j.rser.2020.110340.

[27] M. Liu *et al.*, "Review and characterisation of high-temperature phase change material candidates between 500 C and 700 degrees C," *Renew. Sust. Energ. Rev.,* vol. 150, Oct 2021, Art no. 111528, doi: 10.1016/j.rser.2021.111528.

[28] A. Abhat, "Low temperature latent heat thermal energy storage: heat storage materials," *Sol. Energy,* vol. 30, no. 4, pp. 313-332, 1983.

[29] D. Zhou, C. Y. Zhao, and Y. Tian, "Review on thermal energy storage with phase change materials (PCMs) in building applications," *Appl. Energy,* vol. 92, pp. 593-605, 2012/04/01/ 2012, doi: https://doi.org/10.1016/j.apenergy.2011.08.025.

[30] S. E. Kalnæs and B. P. Jelle, "Phase change materials and products for building applications: A state-of-the-art review and future research opportunities," *Energy Build.,* vol. 94, pp. 150-176, 2015/05/01/ 2015, doi: https://doi.org/10.1016/j.enbuild.2015.02.023.

[31] Z. Khan, Z. Khan, and A. Ghafoor, "A review of performance enhancement of PCM based latent heat storage system within the context of materials, thermal stability and compatibility," *Energy Conversion and Management,* vol. 115, pp. 132-158, 5/1/ 2016, doi: http://dx.doi.org/10.1016/j.enconman.2016.02.045.

[32] A. Frazzica and L. F. Cabeza, *Recent Advancements in Materials and Systems for Thermal Energy Storage: An Introduction to Experimental Characterization Methods*. Springer, 2018.

[33] E. Oró, L. Miró, C. Barreneche, I. Martorell, M. M. Farid, and L. F. Cabeza, "Corrosion of metal and polymer containers for use in PCM cold storage," *Appl. Energy,* vol. 109, pp. 449-453, 2013.

[34] S. Guillot *et al.*, "Corrosion effects between molten salts and thermal storage material for concentrated solar power plants," *Appl. Energy,* vol. 94, pp. 174-181, 2012.

[35] C. Castellón, I. Martorell, L. F. Cabeza, A. I. Fernández, and A. Manich, "Compatibility of plastic with phase change materials (PCM)," *International journal of energy research,* vol. 35, no. 9, pp. 765-771, 2011.

[36] M. K. Rathod and J. Banerjee, "Thermal stability of phase change materials used in latent heat energy storage systems: A review," *Renewable and sustainable energy reviews,* vol. 18, pp. 246-258, 2013.

[37] C. Cárdenas-Ramírez, F. Jaramillo, and M. Gómez, "Systematic review of encapsulation and shape-stabilization of phase change materials," *Journal of Energy Storage,* vol. 30, p. 101495, 2020.

[38] Y. B. Tao and Y.-L. He, "A review of phase change material and performance enhancement method for latent heat storage system," *Renewable and Sustainable Energy Reviews,* vol. 93, pp. 245-259, 2018/10/01/ 2018, doi: https://doi.org/10.1016/j.rser.2018.05.028.

[39] M. Al-Maghalseh and K. Mahkamov, "Methods of heat transfer intensification in PCM thermal storage systems: Review paper," *Renewable and Sustainable Energy Reviews,* vol. 92, pp. 62-94, 2018/09/01/ 2018, doi: https://doi.org/10.1016/j.rser.2018.04.064.

[40] Y. Lin, Y. Jia, G. Alva, and G. Fang, "Review on thermal conductivity enhancement, thermal properties and applications of phase change materials in thermal energy storage," *Renewable and sustainable energy reviews,* vol. 82, pp. 2730-2742, 2018.

[41] L. S. Wong-Pinto, Y. Milian, and S. Ushak, "Progress on use of nanoparticles in salt hydrates as phase change materials," *Renew. Sust. Energ. Rev.,* vol. 122, Apr 2020, Art no. 109727, doi: 10.1016/j.rser.2020.109727.

[42] S. Zhang *et al.*, "A review of phase change heat transfer in shape-stabilized phase change materials (ss-PCMs) based on porous supports for thermal energy storage," *Renew. Sust. Energ. Rev.,* vol. 135, Jan 2021, Art no. 110127, doi: 10.1016/j.rser.2020.110127.

[43] F. Jiang *et al.*, "Skeleton materials for shape-stabilization of high temperature salts based phase change materials: A critical review," *Renew. Sust. Energ. Rev.,* vol. 119, Mar 2020, Art no. 109539, doi: 10.1016/j.rser.2019.109539.

[44] D. L. Feng *et al.*, "Review on nanoporous composite phase change materials: Fabrication, characterization, enhancement and molecular simulation," *Renew. Sust. Energ. Rev.,* vol. 109, pp. 578-605, Jul 2019, doi: 10.1016/j.rser.2019.04.041.

[45] S. D. Zhang and Z. Y. Wang, "Thermodynamics behavior of phase change latent heat materials in micro-/nanoconfined spaces for thermal storage and applications," *Renew. Sust. Energ. Rev.,* vol. 82, pp. 2319-2331, Feb 2018, doi: 10.1016/j.rser.2017.08.080.

[46] A. M. Abdulateef, S. Mat, J. Abdulateef, K. Sopian, and A. A. Al-Abidi, "Geometric and design parameters of fins employed for enhancing thermal energy storage systems: a review,"

Renewable and Sustainable Energy Reviews, vol. 82, pp. 1620-1635, 2018/02/01/ 2018, doi: https://doi.org/10.1016/j.rser.2017.07.009.

[47] M. Kind *et al.*, "VDI Heat Atlas," 2010.

[48] S. Kakac, H. Liu, and A. Pramuanjaroenkij, *Heat exchangers: selection, rating, and thermal design*, Third ed. CRC press, 2012.

[49] L. F. Cabeza, E. Galindo, C. Prieto, C. Barreneche, and A. I. Fernández, "Key performance indicators in thermal energy storage: Survey and assessment," *Renewable Energy,* vol. 83, pp. 820-827, 2015.

[50] J. Fernandez-Seara, F. J. Uhía, J. Sieres, and A. Campo, "A general review of the Wilson plot method and its modifications to determine convection coefficients in heat exchange devices," *Applied Thermal Engineering,* vol. 27, no. 17-18, pp. 2745-2757, 2007.

[51] D. Bauer, "Annex 30: Thermal Energy Storage for Cost-Effective Energy Management and CO2 Mitigation," 2018.

[52] D. Gibb, M. Johnson, J. Romaní, J. Gasia, L. F. Cabeza, and A. Seitz, "Process integration of thermal energy storage systems – Evaluation methodology and case studies," *Appl. Energy,* vol. 230, pp. 750-760, 2018/11/15/ 2018, doi: https://doi.org/10.1016/j.apenergy.2018.09.001.

[53] V. Palomba, A. Frazzica, J. Gasia, and L. F. Cabeza, "Experimental characterization of latent thermal energy storage systems," in *Recent Advancements in Materials and Systems for Thermal Energy Storage*: Springer, 2019, pp. 173-200.

[54] I. Dincer and M. Rosen, *Thermal energy storage: systems and applications*. John Wiley & Sons, 2002.

[55] I. Sarbu and C. Sebarchievici, "A comprehensive review of thermal energy storage," *Sustainability,* vol. 10, no. 1, p. 191, 2018.

[56] L. F. Cabeza, *Advances in thermal energy storage systems: Methods and applications*. Elsevier, 2014.

[57] P. Feng, B. Zhao, and R. Wang, "Thermophysical heat storage for cooling, heating, and power generation: A review," *Applied Thermal Engineering,* vol. 166, p. 114728, 2020.

[58] M. J. Moran, H. N. Shapiro, D. D. Boettner, and M. B. Bailey, *Principles of engineering thermodynamics*. Wiley Global Education, 2015.

[59] J. Welty, G. L. Rorrer, and D. G. Foster, *Fundamentals of momentum, heat, and mass transfer*. John Wiley & Sons, 2014.

[60] B. Zalba, J. M. Marín, L. F. Cabeza, and H. Mehling, "Review on thermal energy storage with phase change: materials, heat transfer analysis and applications," *Applied Thermal Engineering,* vol. 23, no. 3, pp. 251-283, 2// 2003, doi: https://doi.org/10.1016/S1359-4311(02)00192-8.

[61] W. Su, L. Gao, L. Wang, and H. Zhi, "Calibration of differential scanning calorimeter (DSC) for thermal properties analysis of phase change material," *Journal of Thermal Analysis and Calorimetry,* vol. 143, no. 4, pp. 2995-3002, 2021.

[62] J. Tarragona, W. Beyne, A. de Gracia, L. F. Cabeza, and M. De Paepe, "Experimental analysis of a latent thermal energy storage system enhanced with metal foam," *Journal of Energy Storage,* vol. 41, p. 102860, 2021/09/01/ 2021, doi: https://doi.org/10.1016/j.est.2021.102860.

[63] N. H. S. Tay, F. Bruno, and M. Belusko, "Experimental validation of a CFD and an ε-NTU model for a large tube-in-tank PCM system," *Int. J. Heat Mass Transf.,* vol. 55, no. 21, pp. 5931-5940, 2012/10/01/ 2012, doi: http://dx.doi.org/10.1016/j.ijheatmasstransfer.2012.06.004.

[64] A. Trp, "An experimental and numerical investigation of heat transfer during technical grade paraffin melting and solidification in a shell-and-tube latent thermal energy storage unit," *Sol. Energy,* vol. 79, no. 6, pp. 648-660, 2005/12/01/ 2005, doi: https://doi.org/10.1016/j.solener.2005.03.006.

[65] M. Hosseini, A. Ranjbar, K. Sedighi, and M. Rahimi, "A combined experimental and computational study on the melting behavior of a medium temperature phase change storage material inside shell and tube heat exchanger," *International Communications in Heat and Mass Transfer,* vol. 39, no. 9, pp. 1416-1424, 2012.

[66] S. M. J. Hosseini, A. A. Ranjbar, K. Sedighi, and M. Rahimi, "Melting of nanoprticle-enhanced phase change material inside shell and tube heat exchanger," *Journal of Engineering,* vol. 2013, 2013.

[67] S. Thiem, A. Born, V. Danov, A. Vandersickel, J. Schäfer, and T. Hamacher, "Automated identification of a complex storage model and hardware implementation of a model-predictive controller for a cooling system with ice storage," *Applied Thermal Engineering,* vol. 121, pp. 922-940, 2017/07/05/ 2017, doi: https://doi.org/10.1016/j.applthermaleng.2017.04.149.

[68] A. Shahsavar, A. Goodarzi, H. I. Mohammed, A. Shirneshan, and P. Talebizadehsardari, "Thermal performance evaluation of non-uniform fin array in a finned double-pipe latent heat storage system," *Energy,* vol. 193, p. 116800, 2020.

[69] S. Jesumathy, M. Udayakumar, S. Suresh, and S. Jegadheeswaran, "An experimental study on heat transfer characteristics of paraffin wax in horizontal double pipe heat latent heat storage unit," *Journal of the Taiwan Institute of Chemical Engineers,* vol. 45, no. 4, pp. 1298-1306, 2014.

[70] S. S. Ardahaie, M. Hosseini, A. Ranjbar, and M. Rahimi, "Energy storage in latent heat storage of a solar thermal system using a novel flat spiral tube heat exchanger," *Applied Thermal Engineering,* vol. 159, p. 113900, 2019.

[71] R. Elbahjaoui, H. El Qarnia, and A. Naimi, "Thermal performance analysis of combined solar collector with triple concentric-tube latent heat storage systems," *Energy Build.,* vol. 168, pp. 438-456, 2018.

[72] M. H. Abokersh, M. El-Morsi, O. Sharaf, and W. Abdelrahman, "An experimental evaluation of direct flow evacuated tube solar collector integrated with phase change material," *Energy,* vol. 139, pp. 1111-1125, 2017.

[73] W.-W. Wang, L.-B. Wang, and Y.-L. He, "The energy efficiency ratio of heat storage in one shell-and-one tube phase change thermal energy storage unit," *Appl. Energy,* vol. 138, pp. 169-182, 2015/01/15/ 2015, doi: https://doi.org/10.1016/j.apenergy.2014.10.064.

[74] W.-W. Wang, L.-B. Wang, and Y.-L. He, "Parameter effect of a phase change thermal energy storage unit with one shell and one finned tube on its energy efficiency ratio and heat storage rate," *Applied Thermal Engineering,* vol. 93, pp. 50-60, 2016/01/25/ 2016, doi: https://doi.org/10.1016/j.applthermaleng.2015.08.108.

[75] L. Kalapala and J. K. Devanuri, "Influence of Fin Parameters on Melting and Solidification Characteristics of a Conical Shell and Tube Latent Heat Storage Unit," *Journal of Energy Resources Technology,* vol. 144, no. 2, 2021, doi: 10.1115/1.4051300.

[76] Y. Lin, Y. Fan, M. Yu, L. Jiang, and X. Zhang, "Performance investigation on an air source heat pump system with latent heat thermal energy storage," *Energy,* vol. 239, p. 121898, 2022/01/15/ 2022, doi: https://doi.org/10.1016/j.energy.2021.121898.

[77] Y. Pahamli, M. J. Hosseini, S. S. Ardahaie, and A. A. Ranjbar, "Improvement of a phase change heat storage system by Blossom-Shaped Fins: Energy analysis," *Renewable Energy,* vol. 182, pp. 192-215, 2022/01/01/ 2022, doi: https://doi.org/10.1016/j.renene.2021.09.128.

[78] M. J. Moran, H. N. Shapiro, D. D. Boettner, and M. B. Bailey, *Fundamentals of engineering thermodynamics*. John Wiley & Sons, 2010.

[79] G. Zsembinszki, C. Orozco, J. Gasia, T. Barz, J. Emhofer, and L. F. Cabeza, "Evaluation of the state of charge of a solid/liquid phase change material in a thermal energy storage tank," *Energies,* vol. 13, no. 6, p. 1425, 2020.

[80] M. A. Ezan, L. Cetin, and A. Erek, "Ice thickness measurement method for thermal energy storage unit," *Journal of Thermal Science and Technology,* vol. 31, no. 1, pp. 1-10, 2011.
[81] G. Zhou, M. Zhu, and Y. Xiang, "Effect of percussion vibration on solidification of supercooled salt hydrate PCM in thermal storage unit," *Renewable Energy,* vol. 126, pp. 537-544, 2018.
[82] T. Barz *et al.*, "State and state of charge estimation for a latent heat storage," *Control Engineering Practice,* vol. 72, pp. 151-166, 2018.
[83] R. Karami and B. Kamkari, "Experimental investigation of the effect of perforated fins on thermal performance enhancement of vertical shell and tube latent heat energy storage systems," *Energy Conversion and Management,* vol. 210, p. 112679, 2020.
[84] G. Steinmaurer, M. Krupa, and P. Kefer, "Development of sensors for measuring the enthalpy of PCM storage systems," *Energy Procedia,* vol. 48, pp. 440-446, 2014.
[85] L. Navarro, A. de Gracia, A. Castell, S. Álvarez, and L. F. Cabeza, "PCM incorporation in a concrete core slab as a thermal storage and supply system: Proof of concept," *Energy Build.,* vol. 103, pp. 70-82, 9/15/ 2015, doi: https://doi.org/10.1016/j.enbuild.2015.06.028.
[86] D. Laing, C. Bahl, T. Bauer, D. Lehmann, and W.-D. Steinmann, "Thermal energy storage for direct steam generation," *Sol. Energy,* vol. 85, no. 4, pp. 627-633, 2011.
[87] J. Yang, L. Yang, C. Xu, and X. Du, "Experimental study on enhancement of thermal energy storage with phase-change material," *Appl. Energy,* vol. 169, pp. 164-176, 5/1/ 2016, doi: http://dx.doi.org/10.1016/j.apenergy.2016.02.028.
[88] M. K. Rathod and J. Banerjee, "Thermal performance enhancement of shell and tube Latent Heat Storage Unit using longitudinal fins," *Applied thermal engineering,* vol. 75, pp. 1084-1092, 2015.
[89] M. Martinelli, F. Bentivoglio, A. Caron-Soupart, R. Couturier, J.-F. Fourmigue, and P. Marty, "Experimental study of a phase change thermal energy storage with copper foam," *Applied Thermal Engineering,* vol. 101, pp. 247-261, 2016/05/25/ 2016, doi: https://doi.org/10.1016/j.applthermaleng.2016.02.095.
[90] K. Merlin, J. Soto, D. Delaunay, and L. Traonvouez, "Industrial waste heat recovery using an enhanced conductivity latent heat thermal energy storage," *Appl. Energy,* vol. 183, pp. 491-503, 2016/12/01/ 2016, doi: https://doi.org/10.1016/j.apenergy.2016.09.007.
[91] A. Castell, M. Belusko, F. Bruno, and L. F. Cabeza, "Maximisation of heat transfer in a coil in tank PCM cold storage system," *Appl. Energy,* vol. 88, no. 11, pp. 4120-4127, 2011.
[92] M. Kabbara, D. Groulx, and A. Joseph, "Experimental investigations of a latent heat energy storage unit using finned tubes," *Applied Thermal Engineering,* vol. 101, pp. 601-611, 2016.
[93] C. Chen, H. Zhang, X. Gao, T. Xu, Y. Fang, and Z. Zhang, "Numerical and experimental investigation on latent thermal energy storage system with spiral coil tube and paraffin/expanded graphite composite PCM," *Energy conversion and management,* vol. 126, pp. 889-897, 2016.
[94] A. Amini, J. Miller, and H. Jouhara, "An investigation into the use of the heat pipe technology in thermal energy storage heat exchangers," *Energy,* vol. 136, pp. 163-172, 2017.
[95] J. Gasia, J. Diriken, M. Bourke, J. Van Bael, and L. F. Cabeza, "Comparative study of the thermal performance of four different shell-and-tube heat exchangers used as latent heat thermal energy storage systems," *Renewable Energy,* vol. 114, pp. 934-944, 2017.
[96] Z. Khan and Z. A. Khan, "An experimental investigation of discharge/solidification cycle of paraffin in novel shell and tube with longitudinal fins based latent heat storage system," *Energy conversion and management,* vol. 154, pp. 157-167, 2017.
[97] Z. Khan and Z. A. Khan, "Thermodynamic performance of a novel shell-and-tube heat exchanger incorporating paraffin as thermal storage solution for domestic and commercial applications," *Applied Thermal Engineering,* vol. 160, p. 114007, 2019.

[98] Z. Khan and Z. A. Khan, "Experimental and numerical investigations of nano-additives enhanced paraffin in a shell-and-tube heat exchanger: a comparative study," *Applied Thermal Engineering,* vol. 143, pp. 777-790, 2018.
[99] Z. Khan, Z. A. Khan, and P. Sewell, "Heat transfer evaluation of metal oxides based nano-PCMs for latent heat storage system application," *Int. J. Heat Mass Transf.,* vol. 144, p. 118619, 2019.
[100] A. R. Mazhar, S. Liu, and A. Shukla, "Experimental study on the thermal performance of a grey water heat harnessing exchanger using Phase Change Materials," *Renewable Energy,* vol. 146, pp. 1805-1817, 2020.
[101] A. Egea, J. Solano, J. Pérez-García, and A. García, "Solar-driven melting dynamics in a shell and tube thermal energy store: An experimental analysis," *Renewable Energy,* 2020.
[102] M. Esapour, A. Hamzehnezhad, A. A. Rabienataj Darzi, and M. Jourabian, "Melting and solidification of PCM embedded in porous metal foam in horizontal multi-tube heat storage system," *Energy Conversion and Management,* vol. 171, pp. 398-410, 2018/09/01/ 2018, doi: https://doi.org/10.1016/j.enconman.2018.05.086.
[103] A. Reyes, L. Henríquez-Vargas, J. Vásquez, N. Pailahueque, and G. Aguilar, "Analysis of a laboratory scale thermal energy accumulator using two-phases heterogeneous paraffin wax-water mixtures," *Renewable Energy,* vol. 145, pp. 41-51, 2020.
[104] G. S. Sodhi, A. K. Jaiswal, K. Vigneshwaran, and P. Muthukumar, "Investigation of charging and discharging characteristics of a horizontal conical shell and tube latent thermal energy storage device," *Energy Conversion and Management,* vol. 188, pp. 381-397, 2019.
[105] B. D. Mselle, G. Zsembinszki, D. Vérez, E. Borri, and L. F. Cabeza, "A detailed energy analysis of a novel evaporator with latent thermal energy storage ability," *Applied Thermal Engineering,* vol. 201, p. 117844, 2022/01/25/ 2022, doi: https://doi.org/10.1016/j.applthermaleng.2021.117844.
[106] Y. H. Diao, Q. Qin, Z. Y. Wang, Y. H. Zhao, C. Q. Chen, and R. Y. Ren, "Numerical and experimental investigation on a latent heat thermal storage device featuring flat micro heat pipe arrays with offset strip fins," *JOURNAL OF ENERGY STORAGE,* vol. 41, SEP 2021, doi: 10.1016/j.est.2021.102880.
[107] E. F. Akyurek and M. Yoladi, "An experimental investigation on melting and solidification behavior of phase change material in cylindrical latent heat storage units with minichannel," *JOURNAL OF ENERGY STORAGE,* vol. 41, SEP 2021, doi: 10.1016/j.est.2021.102938.
[108] A. Kumar and R. Agrawal, "An experimental investigation of cylindrical shaped thermal storage unit consisting of phase change material based helical coil heat exchanger," *Journal of Energy Storage,* vol. 45, p. 103795, 2022/01/01/ 2022, doi: https://doi.org/10.1016/j.est.2021.103795.
[109] J. Guo, Z. Liu, B. Yang, X. Yang, and J. Yan, "Melting assessment on the angled fin design for a novel latent heat thermal energy storage tube," *Renewable Energy,* vol. 183, pp. 406-422, 2022/01/01/ 2022, doi: https://doi.org/10.1016/j.renene.2021.11.007.
[110] T. Pekdogan, A. Tokuç, M. A. Ezan, and T. Başaran, "Experimental investigation on heat transfer and air flow behavior of latent heat storage unit in a facade integrated ventilation system," *Journal of Energy Storage,* vol. 44, p. 103367, 2021/12/01/ 2021, doi: https://doi.org/10.1016/j.est.2021.103367.
[111] K. Nedjem, M. Teggar, T. Hadibi, M. Arıcı, Ç. Yıldız, and K. A. R. Ismail, "Hybrid thermal performance enhancement of shell and tube latent heat thermal energy storage using nano-additives and metal foam," *Journal of Energy Storage,* vol. 44, p. 103347, 2021/12/01/ 2021, doi: https://doi.org/10.1016/j.est.2021.103347.
[112] X. Jin, H. Zhang, G. Huang, and A. C. K. Lai, "Experimental investigation on the dynamic thermal performance of the parallel solar-assisted air-source heat pump latent heat thermal energy storage system," *Renewable Energy,* vol. 180, pp. 637-657, 2021/12/01/ 2021, doi: https://doi.org/10.1016/j.renene.2021.08.067.

[113] C. Zeng *et al.*, "Operating performance of multi-modular water-phase change material tanks for emergency cooling in an underground shelter," *International Journal of Energy Research,* 2021.
[114] G. S. Sodhi, K. Vigneshwaran, and P. Muthukumar, "Experimental investigations of high-temperature shell and multi-tube latent heat storage system," *Applied Thermal Engineering,* vol. 198, p. 117491, 2021/11/05/ 2021, doi: https://doi.org/10.1016/j.applthermaleng.2021.117491.
[115] H. İ. Yamaç and A. Koca, "Experimental investigation of water flow window system and numerical modeling of solar thermal energy storage with phase change materials on the way of nearly zero energy buildings," *Journal of Energy Storage,* vol. 43, p. 103118, 2021/11/01/ 2021, doi: https://doi.org/10.1016/j.est.2021.103118.
[116] H. Selvnes, Y. Allouche, and A. Hafner, "Experimental characterisation of a cold thermal energy storage unit with a pillow-plate heat exchanger design," *Applied Thermal Engineering,* vol. 199, p. 117507, 2021/11/25/ 2021, doi: https://doi.org/10.1016/j.applthermaleng.2021.117507.
[117] M. Fadl and P. C. Eames, "Thermal performance evaluation of a latent heat thermal energy storage unit with an embedded multi-tube finned copper heat exchanger," *Experimental Heat Transfer,* pp. 1-20, 2021.
[118] H. Koide *et al.*, "Performance analysis of packed bed latent heat storage system for high-temperature thermal energy storage using pellets composed of micro-encapsulated phase change material," *Energy,* vol. 238, p. 121746, 2022/01/01/ 2022, doi: https://doi.org/10.1016/j.energy.2021.121746.
[119] N. H. S. Tay, F. Bruno, and M. Belusko, "Comparison of pinned and finned tubes in a phase change thermal energy storage system using CFD," *Appl. Energy,* vol. 104, pp. 79-86, 2013/04/01/ 2013, doi: https://doi.org/10.1016/j.apenergy.2012.10.040.
[120] J. S. Prasad, P. Muthukumar, R. Anandalakshmi, and H. Niyas, "Comparative study of phase change phenomenon in high temperature cascade latent heat energy storage system using conduction and conduction-convection models," *Sol. Energy,* vol. 176, pp. 627-637, 2018.
[121] W. Lin, R. Huang, X. Fang, and Z. Zhang, "Improvement of thermal performance of novel heat exchanger with latent heat storage," *Int. J. Heat Mass Transf.,* vol. 140, pp. 877-885, 2019.
[122] M. Parsazadeh and X. Duan, "Numerical study on the effects of fins and nanoparticles in a shell and tube phase change thermal energy storage unit," *Appl. Energy,* vol. 216, pp. 142-156, 2018.
[123] A. Reyes, L. Henríquez-Vargas, R. Aravena, and F. Sepúlveda, "Experimental analysis, modeling and simulation of a solar energy accumulator with paraffin wax as PCM," *Energy Conversion and Management,* vol. 105, pp. 189-196, 2015.
[124] H. Moon, N. Miljkovic, and W. P. King, "High power density thermal energy storage using additively manufactured heat exchangers and phase change material," *Int. J. Heat Mass Transf.,* vol. 153, p. 119591, 2020.
[125] X. Sun, J. M. Mahdi, H. I. Mohammed, H. S. Majdi, W. Zixiong, and P. Talebizadehsardari, "Solidification Enhancement in a Triple-Tube Latent Heat Energy Storage System Using Twisted Fins," *Energies,* vol. 14, no. 21, p. 7179, 2021.
[126] X. Zhang, M. Xu, L. Liu, Q. Yang, and K. I. Song, "Study on thermal performance of casing-type mine heat recovery device with phase change materials filling in annular space," *International Journal of Energy Research,* vol. 45, no. 12, pp. 17577-17596, 2021.
[127] M. Ali, A. K. Alkaabi, and Y. Addad, "Numerical investigation of a vertical triplex-tube latent heat storage/exchanger to achieve flexible operation of nuclear power plants," *International Journal of Energy Research,* vol. 46, no. 3, pp. 2970-2987, Mar 2022, doi: 10.1002/er.7357.
[128] X. G. Sun *et al.*, "Investigation of Heat Transfer Enhancement in a Triple Tube Latent Heat Storage System Using Circular Fins with Inline and Staggered Arrangements," *NANOMATERIALS,* vol. 11, no. 10, OCT 2021, doi: 10.3390/nano11102647.

[129] A. Chibani, S. Merouani, and F. Benmoussa, "Computational analysis of the melting process of Phase change material-metal foam-based latent thermal energy storage unit: The heat exchanger configuration," *JOURNAL OF ENERGY STORAGE,* vol. 42, OCT 2021, doi: 10.1016/j.est.2021.103071.
[130] R. Elbahjaoui, "Improvement of the thermal performance of a solar triple concentric-tube thermal energy storage unit using cascaded phase change materials," *JOURNAL OF ENERGY STORAGE,* vol. 42, OCT 2021, doi: 10.1016/j.est.2021.103047.
[131] A. H. Eisapour, M. Eisapour, H. I. Mohammed, A. H. Shafaghat, M. Ghalambaz, and P. Talebizadehsardari, "Optimum design of a double elliptical latent heat energy storage system during the melting process," *Journal of Energy Storage,* vol. 44, p. 103384, 2021/12/01/ 2021, doi: https://doi.org/10.1016/j.est.2021.103384.
[132] G. S. Sodhi, V. Kumar, and P. Muthukumar, "Design assessment of a horizontal shell and tube latent heat storage system: Alternative to fin designs," *Journal of Energy Storage,* vol. 44, p. 103282, 2021/12/01/ 2021, doi: https://doi.org/10.1016/j.est.2021.103282.
[133] M. Z. Mahmoud *et al.*, "Melting Enhancement in a Triple-Tube Latent Heat Storage System with Sloped Fins," *Nanomaterials,* vol. 11, no. 11, p. 3153, 2021.
[134] Z. Elmaazouzi, I. A. Laasri, A. Gounni, M. E. Alami, and E. G. Bennouna, "Enhanced thermal performance of finned latent heat thermal energy storage system: fin parameters optimization," *Journal of Energy Storage,* vol. 43, p. 103116, 2021/11/01/ 2021, doi: https://doi.org/10.1016/j.est.2021.103116.
[135] G. S. Sau *et al.*, "High-Temperature Chloride-Carbonate Phase Change Material: Thermal Performances and Modelling of a Packed Bed Storage System for Concentrating Solar Power Plants," *ENERGIES,* vol. 14, no. 17, SEP 2021, doi: 10.3390/en14175339.
[136] K. Chen, H. I. Mohammed, J. M. Mahdi, A. Rahbari, A. Cairns, and P. Talebizadehsardari, "Effects of non-uniform fin arrangement and size on the thermal response of a vertical latent heat triple-tube heat exchanger," *Journal of Energy Storage,* vol. 45, p. 103723, 2022/01/01/ 2022, doi: https://doi.org/10.1016/j.est.2021.103723.
[137] A. Trp, K. Lenic, and B. Frankovic, "Analysis of the influence of operating conditions and geometric parameters on heat transfer in water-paraffin shell-and-tube latent thermal energy storage unit," *Applied Thermal Engineering,* vol. 26, no. 16, pp. 1830-1839, 2006/11/01/ 2006, doi: https://doi.org/10.1016/j.applthermaleng.2006.02.004.
[138] K. A. R. Ismail, O. C. Quispe, and J. R. Henríquez, "A numerical and experimental study on a parallel plate ice bank," *Applied Thermal Engineering,* vol. 19, no. 2, pp. 163-193, 1999/02/01/ 1999, doi: https://doi.org/10.1016/S1359-4311(98)00024-6.
[139] J. Gasia, A. de Gracia, G. Zsembinszki, and L. F. Cabeza, "Influence of the storage period between charge and discharge in a latent heat thermal energy storage system working under partial load operating conditions," *Appl. Energy,* vol. 235, pp. 1389-1399, 2019/02/01/ 2019, doi: https://doi.org/10.1016/j.apenergy.2018.11.041.
[140] Y. Shen, Y. Liu, S. Liu, and A. R. Mazhar, "A dynamic method to optimize cascaded latent heat storage systems with a genetic algorithm: A case study of cylindrical concentric heat exchanger," *Int. J. Heat Mass Transf.,* vol. 183, p. 122051, 2022/02/01/ 2022, doi: https://doi.org/10.1016/j.ijheatmasstransfer.2021.122051.
[141] M. Medrano, M. O. Yilmaz, M. Nogués, I. Martorell, J. Roca, and L. F. Cabeza, "Experimental evaluation of commercial heat exchangers for use as PCM thermal storage systems," *Appl. Energy,* vol. 86, no. 10, pp. 2047-2055, 2009/10/01/ 2009, doi: https://doi.org/10.1016/j.apenergy.2009.01.014.

[142] M. Belusko, N. H. S. Tay, M. Liu, and F. Bruno, "Effective tube-in-tank PCM thermal storage for CSP applications, Part 1: Impact of tube configuration on discharging effectiveness," *Sol. Energy,* vol. 139, pp. 733-743, 2016/12/01/ 2016, doi: https://doi.org/10.1016/j.solener.2015.09.042.
[143] Z. N. Meng and P. Zhang, "Experimental and numerical investigation of a tube-in-tank latent thermal energy storage unit using composite PCM," *Appl. Energy,* vol. 190, pp. 524-539, 2017/03/15/ 2017, doi: https://doi.org/10.1016/j.apenergy.2016.12.163.
[144] A. Shinde, S. Arpit, P. KM, P. V. C. Rao, and S. K. Saha, "Heat transfer characterization and optimization of latent heat thermal storage system using fins for medium temperature solar applications," *Journal of Solar Energy Engineering,* vol. 139, no. 3, 2017.
[145] N. A. M. Amin, F. Bruno, and M. Belusko, "Effectiveness–NTU correlation for low temperature PCM encapsulated in spheres," *Appl. Energy,* vol. 93, pp. 549-555, 2012/05/01/ 2012, doi: https://doi.org/10.1016/j.apenergy.2011.12.006.
[146] A. López-Navarro *et al.*, "Performance characterization of a PCM storage tank," *Appl. Energy,* vol. 119, pp. 151-162, 2014/04/15/ 2014, doi: https://doi.org/10.1016/j.apenergy.2013.12.041.
[147] M. E. H. Amagour, A. Rachek, M. Bennajah, and M. Ebn Touhami, "Experimental investigation and comparative performance analysis of a compact finned-tube heat exchanger uniformly filled with a phase change material for thermal energy storage," *Energy Conversion and Management,* vol. 165, pp. 137-151, 2018/06/01/ 2018, doi: https://doi.org/10.1016/j.enconman.2018.03.041.
[148] Y. Allouche, S. Varga, C. Bouden, and A. C. Oliveira, "Experimental determination of the heat transfer and cold storage characteristics of a microencapsulated phase change material in a horizontal tank," *Energy Conversion and Management,* vol. 94, pp. 275-285, 2015/04/01/ 2015, doi: https://doi.org/10.1016/j.enconman.2015.01.064.
[149] A. Gil, E. Oró, A. Castell, and L. F. Cabeza, "Experimental analysis of the effectiveness of a high temperature thermal storage tank for solar cooling applications," *Applied Thermal Engineering,* vol. 54, no. 2, pp. 521-527, 2013/05/30/ 2013, doi: https://doi.org/10.1016/j.applthermaleng.2013.02.016.
[150] X. Chen, M. Worall, S. Omer, Y. Su, and S. Riffat, "Experimental investigation on PCM cold storage integrated with ejector cooling system," *Applied Thermal Engineering,* vol. 63, no. 1, pp. 419-427, 2014/02/05/ 2014, doi: https://doi.org/10.1016/j.applthermaleng.2013.11.029.
[151] R. E. Murray and D. Groulx, "Experimental study of the phase change and energy characteristics inside a cylindrical latent heat energy storage system: Part 1 consecutive charging and discharging," *Renewable Energy,* vol. 62, pp. 571-581, 2014/02/01/ 2014, doi: https://doi.org/10.1016/j.renene.2013.08.007.
[152] W. Beyne, K. Couvreur, I. T'Jollyn, R. Tassenoy, S. Lecompte, and M. De Paepe, "A charging time energy fraction method for evaluating the performance of a latent thermal energy storage heat exchanger," *Applied Thermal Engineering,* p. 117068, 2021.
[153] M. Belusko, E. Halawa, and F. Bruno, "Characterising PCM thermal storage systems using the effectiveness-NTU approach," *Int. J. Heat Mass Transf.,* vol. 55, no. 13, pp. 3359-3365, 2012/06/01/ 2012, doi: https://doi.org/10.1016/j.ijheatmasstransfer.2012.03.018.
[154] W. Beyne, K. Couvreur, I. T'Jollyn, S. Lecompte, and M. De Paepe, "Estimating the state of charge in a latent thermal energy storage heat exchanger based on inlet/outlet and surface measurements," *Applied Thermal Engineering,* p. 117806, 2021.
[155] H. El-Dessouky and F. Al-Juwayhel, "Effectiveness of a thermal energy storage system using phase-change materials," *Energy Conversion and Management,* vol. 38, no. 6, pp. 601-617, 1997/04/01/ 1997, doi: https://doi.org/10.1016/S0196-8904(96)00072-6.
[156] M. Belusko, S. Sheoran, and F. Bruno, "Effectiveness of direct contact PCM thermal storage with a gas as the heat transfer fluid," *Appl. Energy,* vol. 137, pp. 748-757, 2015/01/01/ 2015, doi: https://doi.org/10.1016/j.apenergy.2014.06.004.

[157] M. Belusko, N. H. S. Tay, M. Liu, and F. Bruno, "Effective tube-in-tank PCM thermal storage for CSP applications, Part 2: Parametric assessment and impact of latent fraction," *Sol. Energy,* vol. 139, pp. 744-756, 2016/12/01/ 2016, doi: https://doi.org/10.1016/j.solener.2015.09.034.
[158] N. H. S. Tay, F. Bruno, and M. Belusko, "Experimental validation of a CFD model for tubes in a phase change thermal energy storage system," *Int. J. Heat Mass Transf.,* vol. 55, no. 4, pp. 574-585, 2012/01/31/ 2012, doi: https://doi.org/10.1016/j.ijheatmasstransfer.2011.10.054.
[159] N. H. S. Tay, M. Belusko, and F. Bruno, "Experimental investigation of tubes in a phase change thermal energy storage system," *Appl. Energy,* vol. 90, no. 1, pp. 288-297, 2012/02/01/ 2012, doi: https://doi.org/10.1016/j.apenergy.2011.05.026.
[160] A. Sari and K. Kaygusuz, "Thermal performance of palmitic acid as a phase change energy storage material," *Energy Conversion and Management,* vol. 43, no. 6, pp. 863-876, 2002/04/01/ 2002, doi: https://doi.org/10.1016/S0196-8904(01)00071-1.
[161] N. H. S. Tay, M. Belusko, and F. Bruno, "An effectiveness-NTU technique for characterising tube-in-tank phase change thermal energy storage systems," *Appl. Energy,* vol. 91, no. 1, pp. 309-319, 3// 2012, doi: http://dx.doi.org/10.1016/j.apenergy.2011.09.039.
[162] S. W. Churchill and H. H. S. Chu, "Correlating equations for laminar and turbulent free convection from a horizontal cylinder," *Int. J. Heat Mass Transf.,* vol. 18, no. 9, pp. 1049-1053, 1975/09/01/ 1975, doi: http://dx.doi.org/10.1016/0017-9310(75)90222-7.
[163] Y. Zhang, S. Liu, L. Yang, X. Yang, Y. Shen, and X. Han, "Experimental Study on the Strengthen Heat Transfer Performance of PCM by Active Stirring," *Energies,* vol. 13, no. 9, p. 2238, 2020.
[164] J. Gasia, J. M. Maldonado, F. Galati, M. De Simone, and L. F. Cabeza, "Experimental evaluation of the use of fins and metal wool as heat transfer enhancement techniques in a latent heat thermal energy storage system," *Energy Conversion and Management,* vol. 184, pp. 530-538, 2019.
[165] S. Kuboth, A. König-Haagen, and D. Brüggemann, "Numerical analysis of shell-and-tube type latent thermal energy storage performance with different arrangements of circular fins," *Energies,* vol. 10, no. 3, p. 274, 2017.
[166] M. M. Joybari, F. Haghighat, S. Seddegh, and A. A. Al-Abidi, "Heat transfer enhancement of phase change materials by fins under simultaneous charging and discharging," *Energy Conversion and Management,* vol. 152, pp. 136-156, 2017.
[167] W. Youssef, Y. Ge, and S. Tassou, "CFD modelling development and experimental validation of a phase change material (PCM) heat exchanger with spiral-wired tubes," *Energy conversion and management,* vol. 157, pp. 498-510, 2018.
[168] J. R. Patel and M. K. Rathod, "Thermal performance enhancement of melting and solidification process of phase-change material in triplex tube heat exchanger using longitudinal fins," *Heat Transfer—Asian Research,* vol. 48, no. 2, pp. 483-501, 2019.
[169] P. T. Sardari, D. Grant, D. Giddings, G. S. Walker, and M. Gillott, "Composite metal foam/PCM energy store design for dwelling space air heating," *Energy Conversion and Management,* vol. 201, p. 112151, 2019.
[170] C. Zhang, Y. Fan, M. Yu, X. Zhang, and Y. Zhao, "Performance evaluation and analysis of a vertical heat pipe latent thermal energy storage system with fins-copper foam combination," *Applied Thermal Engineering,* vol. 165, p. 114541, 2020/01/25/ 2020, doi: https://doi.org/10.1016/j.applthermaleng.2019.114541.
[171] R. Raud *et al.*, "Design optimization method for tube and fin latent heat thermal energy storage systems," *Energy,* vol. 134, pp. 585-594, 2017.
[172] T. Bauer, "Approximate analytical solutions for the solidification of PCMs in fin geometries using effective thermophysical properties," *Int. J. Heat Mass Transf.,* vol. 54, no. 23, pp. 4923-4930, 2011/11/01/ 2011, doi: https://doi.org/10.1016/j.ijheatmasstransfer.2011.07.004.

[173] W. Beyne, S. Lecompte, B. Ameel, D. Daenens, M. Van Belleghem, and M. De Paepe, "Dynamic and steady state performance model of fire tube boilers with different turn boxes," *Applied Thermal Engineering,* vol. 149, pp. 1454-1462, 2019.
[174] R. K. Shah and D. P. Sekulic, *Fundamentals of heat exchanger design*. John Wiley & Sons, 2003.
[175] W. Beyne, K. Couvreur, I. T'Jollyn, R. Tassenoy, S. Lecompte, and M. De Paepe, "A charging time energy fraction method for evaluating the performance of a latent thermal energy storage heat exchanger," *Applied Thermal Engineering,* vol. 195, p. 117068, 2021.